Detrital zircon provenance of the Late Cretaceous–Eocene California forearc: Influence of Laramide low-angle subduction on sediment dispersal and paleogeography

Glenn R. Sharman[1,†], Stephan A. Graham[1], Marty Grove[1], David L. Kimbrough[2], and James E. Wright[3]
[1]*Department of Geological and Environmental Sciences, Stanford University, Stanford, California 94305, USA*
[2]*Department of Geological Sciences, San Diego State University, San Diego, California 92182, USA*
[3]*Department of Geology, University of Georgia, Athens, Georgia 30602, USA*

ABSTRACT

Upper Cretaceous–Eocene forearc strata deposited along the California continental margin record a complex history of plate convergence that shaped the tectonic development of the U.S. Cordillera. Synthesis of new and published detrital zircon U-Pb ages over a 2000 km length of the southern Oregon–California–northern Baja forearc clearly demonstrates spatial and temporal changes in sandstone provenance that reflect evolving sediment dispersal patterns associated with the extinction of continental margin arc magmatism and transfer of deformation to the continental interior during latest Cretaceous–early Cenozoic Laramide low-angle subduction.

Measured age distributions from Cenomanian to Campanian forearc strata indicate the existence of a drainage divide formed by a high-standing mid-Cretaceous Cordilleran arc that crosscut older, Late Permian–Jurassic arc segments. Progressive influx of 125–85 Ma detrital zircon in the Great Valley forearc reflects ongoing denudation of the Sierra Nevada batholith throughout Late Cretaceous–early Paleogene time. In contrast, age distributions in the Peninsular Ranges forearc indicate early denudation of the Peninsular Ranges batholith that is hypothesized to have resulted from the initial collision of an oceanic plateau with the southern California margin; as a result, these age distributions exhibit little change over time until delivery of extraregional detritus to the margin in Eocene time. Maastrichtian through middle Eocene strata preserved south of the Sierra Nevada record a pronounced shift from local to extraregional provenance caused by the development of drainages that extended across the breached mid-Cretaceous continental margin batholith to tap the continental interior. This geomorphic breaching of the mid-Cretaceous arc, and associated inland drainage migration, represents the culminating influence of Laramide low-angle subduction on the continental margin and likely occurred following subduction of the Shatsky conjugate plateau beneath the western United States.

INTRODUCTION

The Cretaceous–Paleogene forearc of California is perhaps one of the best-studied examples of sedimentation in a convergent setting (e.g., Dickinson, 1995a) and preserves a detailed record of the complex history of plate convergence that has shaped the tectonic development of the U.S. Cordillera. Cretaceous to Paleogene subduction of the Farallon plate beneath North America is recorded in the Sierran–Peninsular Ranges batholith (remnant magmatic arc), adjacent forearc basins, and Franciscan subduction complex (Fig. 1). Together, these elements comprise a type example of a cross section through an ancient convergent margin (Dickinson, 1995a).

The California margin also contains one of the best-preserved records of low-angle slab subduction, associated subduction erosion, and tectonic underplating of the margin batholith (Grove et al., 2003a; Saleeby, 2003; Grove et al., 2008; Ducea et al., 2009; Jacobson et al., 2011; Chapman et al., 2013). This episode of latest Cretaceous–Paleogene low-angle subduction has been widely linked with the development of the Laramide orogeny in the western U.S. Cordillera (Dickinson and Snyder, 1978; Miller et al., 1992) and may have resulted from subduction of thickened oceanic crust (Livaccari et al., 1981; Henderson et al., 1984; Saleeby, 2003; Liu et al., 2010). Because low-angle subduction is a widely occurring phenomenon along convergent margins (Gutscher et al., 2000), the California margin provides an important ancient example of the influence of low-angle subduction on forearc sedimentation and provides valuable insight into arc-forearc dynamics in analogous tectonic settings (e.g., Laursen et al., 2002; Fildani et al., 2008).

Although the Laramide orogeny is well understood to have been manifested in the Cordilleran foreland as a series of basement-cored uplifts and partitioned foreland depocenters (DeCelles, 2004), significant debate exists regarding the influence of this tectonic event on the continental margin (e.g., Saleeby, 2003; Jacobson et al., 2011). Margin tectonism attributed to the Laramide orogeny includes (1) ca. 85 Ma cessation of magmatism in the Sierran–Peninsular Ranges arc accompanied by inland migration of plutonism in the southwestern United States (Chen and Moore, 1982; Lipman, 1992); (2) uplift and denudation of the mid-Cretaceous arc and an associated pulse of forearc sedimentation (Grove et al., 2003b, 2008; Saleeby et al., 2010); (3) uplift and shoaling of the forearc and adjacent subduction complex (Moxon and Graham, 1987; Mitchell et al., 2010); (4) underplating of the subduction complex beneath the southern California segment of the Cordilleran arc (Jacobson et al., 1996; Grove et al., 2003a, 2008); and (5) deep exhumation and structural juxtaposition of the eastern portion of the mid-Cretaceous batholith against the Franciscan subduction complex across the Nacimiento fault (Hall, 1991; Saleeby, 2003; Dickinson et al., 2005; Ducea et al., 2009).

Our approach is to use sedimentary provenance of forearc sandstone to interpret the evolution of Late Cretaceous–Eocene sediment dispersal patterns to the southern Oregon–Cali-

†E-mail: gsharman@stanford.edu.

GSA Bulletin; doi: 10.1130/B31065.1; 8 figures; 1 table; Data Repository item 2014263.

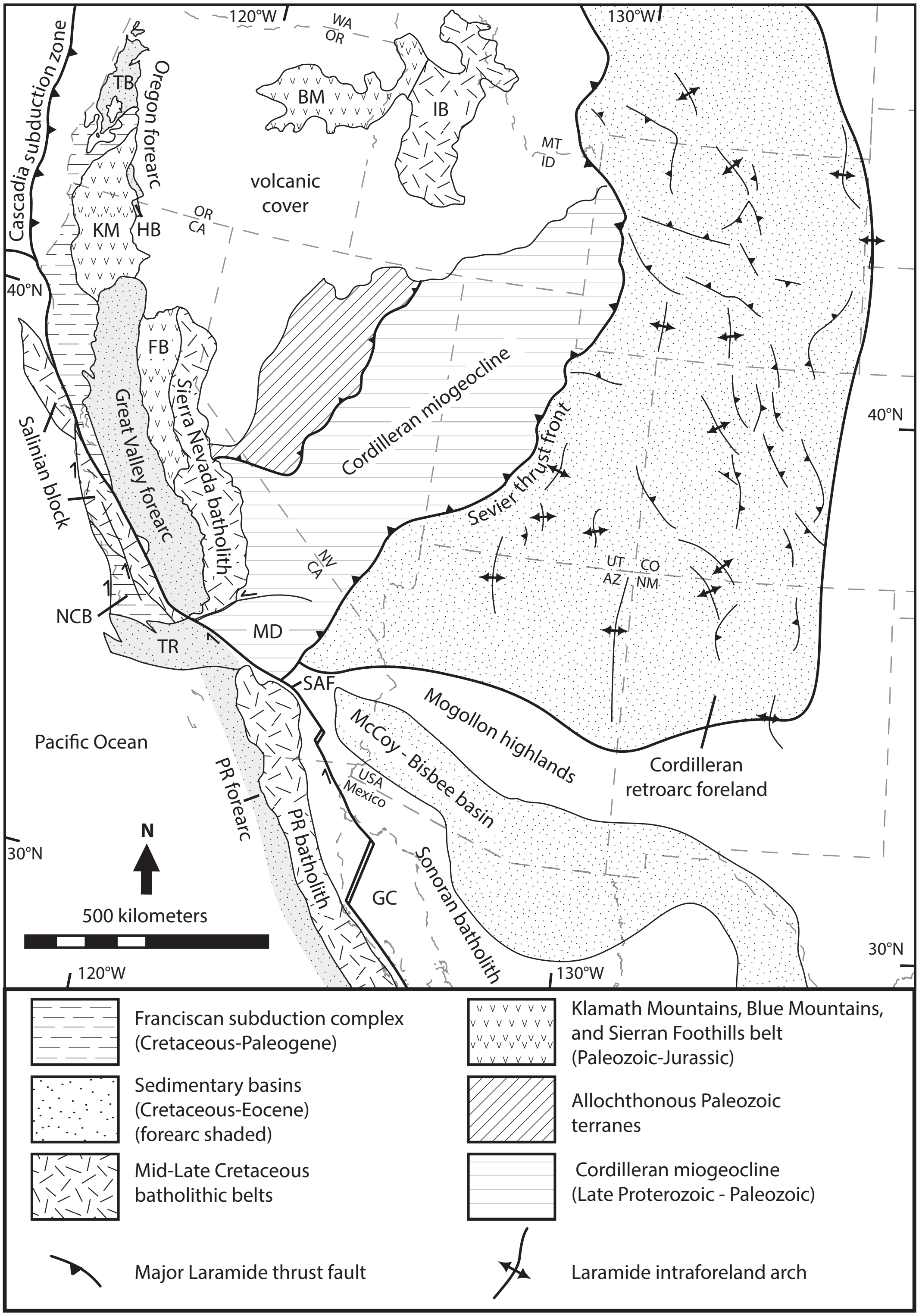

Figure 1. Tectonic setting of the western United States (modified from Dickinson, 1996, 2008; DeCelles, 2004; Grove et al., 2008; Dickinson and Gehrels, 2008; Surpless and Beverly, 2013). BM—Blue Mountains; FB—Foothills belt; GC—Gulf of California; HB—Hornbrook basin; IB—Idaho batholith; KM—Klamath Mountains; MD—Mojave Desert; NCB—Nacimiento block; PR—Peninsular Ranges; SAF—San Andreas fault; TB—Tyee basin; TR—Transverse Ranges.

fornia–northern Baja forearc (hereafter "California forearc") and to consider the influence of Laramide low-angle subduction on margin paleogeography and landscape evolution. In particular, we use detrital zircon U-Pb age distributions to refine previous interpretations based on sandstone petrography, conglomerate clast assemblages, and paleocurrent distributions (e.g., Nilsen and Clarke, 1975; Dickinson et al., 1979; Kies and Abbott, 1982; Ingersoll, 1983; Seiders and Cox, 1992). Because the age distribution of igneous rocks in California is generally well known (e.g., Irwin and Wooden, 2001; Fig. 2), detrital zircon U-Pb ages can be directly linked with potential source regions. Detrital zircon provenance analysis has already been used effectively to improve understanding of drainage evolution along certain segments of

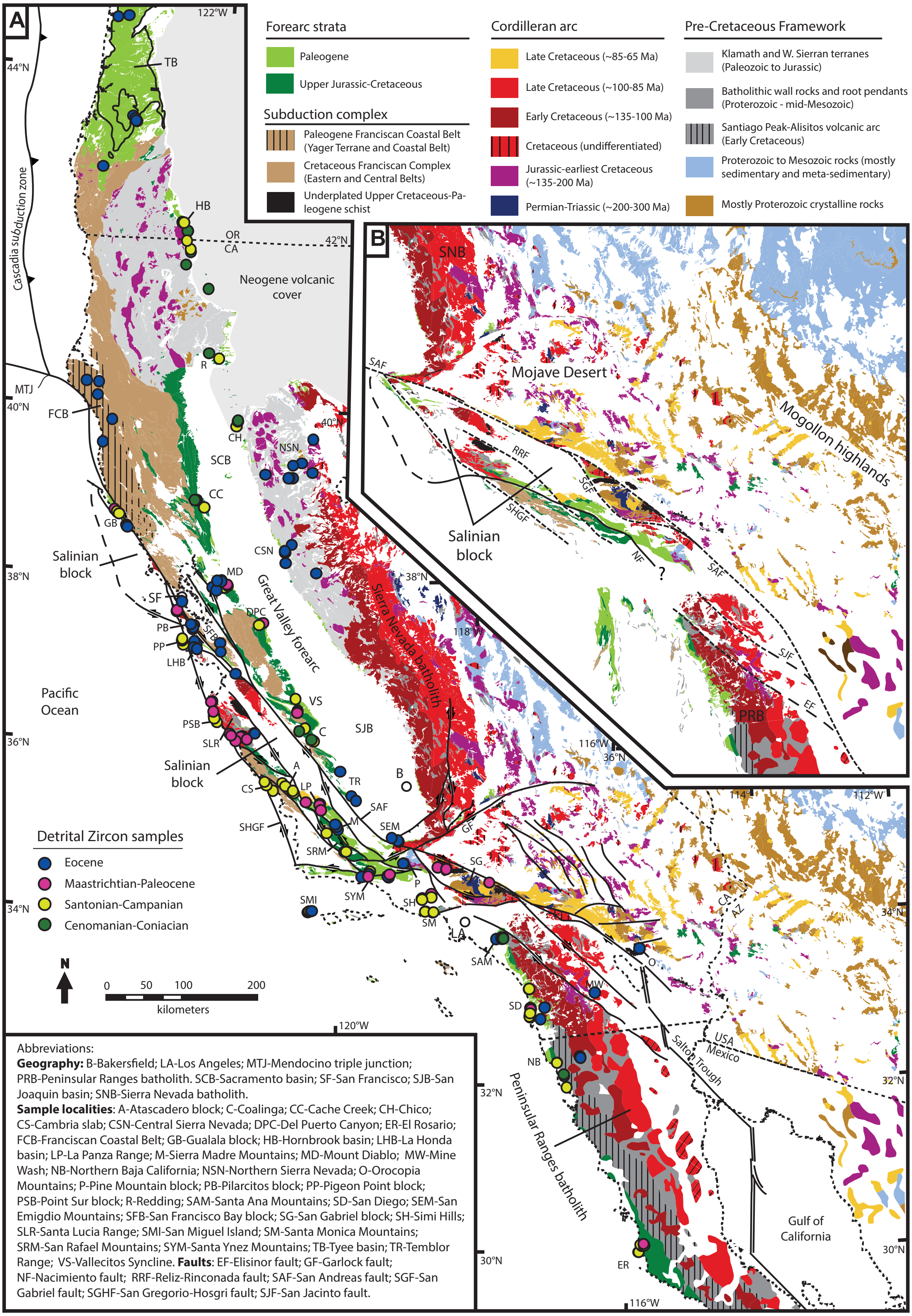

Figure 2. (A) Generalized geologic framework of southern Oregon, California, and northern Baja California. See Appendix DR1 for an explanation of data sources (text footnote 1). (B) Palinspastic reconstruction of southern California–northern Baja California during Eocene time (see text and Appendix DR2 for details [text footnote 1]).

the margin (e.g., DeGraaff-Surpless et al., 2002; Cassel et al., 2012). This study expands on previous work by integrating both new and published U-Pb ages of forearc strata along ~2000 km of the continental margin (Fig. 2). In addition, we consider data sets from time-equivalent units, including the Franciscan subduction complex (Dumitru et al., 2010, 2012; Snow et al., 2010), underplated schist (Grove et al., 2003a, 2008; Jacobson et al., 2011; Chapman et al., 2013), and intra-arc and retroarc foreland basin strata (Barth et al., 2004; Dickinson and Gehrels, 2008; Lechler and Niemi, 2011; Laskowski et al., 2013). By considering regional-scale, spatial trends in sedimentary provenance from Late Cretaceous to Eocene time, we document forearc drainages that progressively migrated inland in response to a redistribution of topography associated with the subduction of an oceanic plateau beneath the continental interior. As such, we place the forearc sedimentary record within the context of an evolving tectonic framework associated with the development of Laramide low-angle subduction.

GEOLOGIC BACKGROUND

Cordilleran Magmatism

A magmatic arc developed along the western U.S. continental margin during Late Permian time and continued throughout the Mesozoic with episodes of increased magmatism occurring during Middle to Late Jurassic (ca. 175–155 Ma) and mid-Cretaceous (ca. 125–85 Ma) time (Figs. 1 and 2; Ducea, 2001; Walker et al., 2002; Ducea and Barton, 2007; Barton et al., 2011). The Jurassic arc that extended along the margin from northwestern Nevada to Sonora, Mexico, was likely a low-standing topographic feature that was dominantly emplaced in an extensional setting (Fig. 2; Walker et al., 2002; Barton et al., 2011) and was incapable of shielding the continental margin from detritus transported from retroarc regions (Ingersoll et al., 2013). Triassic and Jurassic magmatism also occurred in intraoceanic island arcs that were accreted to the margin by Late Jurassic time in the Klamath Mountains and Foothills belt of the western Sierra Nevada (Figs. 1 and 2; Schweickert and Cowan, 1975; Dickinson, 2008).

Voluminous magmatism during mid-Cretaceous time (ca. 125–85 Ma) coincided with the culmination of the Sevier orogeny and likely resulted in a physiography that resembled the modern Andes, with a high-standing volcano-plutonic arc, inboard elevated plateau, and a retroarc fold-and-thrust belt (Figs. 1 and 2; Ducea, 2001; House et al., 2001; DeCelles, 2004). A systematic eastward younging of pluton crystallization ages in the mid-Cretaceous arc reflects progressive migration of magmatism over time associated with gradual slab flattening (Chen and Moore, 1982; Silver and Chappell, 1988). As a result, the Sierran–Peninsular Ranges arc can be divided into eastern and western zones that are separated by a 100 Ma isochron (Fig. 2). Particularly high rates of magmatic flux occurred during Late Cretaceous time that resulted in the Sierra Crest intrusive event (ca. 100–85 Ma) in the Sierra Nevada and emplacement of the La Posta suite (99–92 Ma) in the Peninsular Ranges (Walawender et al., 1990; Coleman and Glazner, 1997; Ducea, 2001; Grove et al., 2003b; Todd et al., 2003; Ducea and Barton, 2007; Coleman et al., 2012). Following extinction of the Sierran–Peninsular Ranges arc, plutonism migrated inland in the southwestern United States and in Sonora, Mexico, and continued throughout latest Cretaceous time (ca. 85–65 Ma; Fig. 2; Lipman, 1992; McDowell et al., 2001).

Tectonic Restructuring of the Southern California Margin

During late Campanian–early Paleogene time, the southern California margin underwent a fundamental restructuring that resulted in the destruction of the topographic continuity of the formerly high-standing mid-Cretaceous arc (Saleeby, 2003; Jacobson et al., 2011; Hall and Saleeby, 2013). The manifestations of this tectonism are most clearly observed where portions of the eastern mid-Cretaceous batholith (e.g., Salinian block) are positioned adjacent to the Franciscan subduction complex across the Nacimiento fault in central California (Figs. 1 and 2; Dickinson, 1983). By analogy to the Sierra Nevada batholith–Great Valley forearc–Franciscan complex triad preserved to the north, this juxtaposition implies removal of 150–180 km of intervening western batholith, foothills belt, and forearc basin (Dickinson et al., 2005).

Two competing models have been proposed to explain this tectonic restructuring of the latest Cretaceous continental margin: (1) large-magnitude (~600–500 km) sinistral displacement along the Nacimiento fault (Dickinson, 1983; Jacobson et al., 2011), or (2) west-directed low-angle faulting of the mid-Cretaceous batholith (Hall, 1991; Barth et al., 2003; Saleeby, 2003; Hall and Saleeby, 2013). Both models are interpreted as manifestations of the collision of an oceanic ridge or plateau with the continental margin associated with the development of the Laramide orogeny (Saleeby, 2003; Jacobson et al., 2011). The Laramide orogeny also coincided with (1) marine transgression that occurred atop deeply denuded batholithic rocks of the southernmost Sierra-Salinian-Mojave segment of the margin (Cox, 1982; Grove, 1993; Kidder et al., 2003; Ducea et al., 2009), and (2) a sudden influx of inboard detritus to the trench and forearc strata preserved atop and adjacent to the Salinian-Mojave segment of the Cretaceous arc (Jacobson et al., 2011).

Upper Cretaceous–Eocene Forearc

A well-defined forearc basin developed by latest Jurassic–earliest Cretaceous time along much of the continental margin (Dickinson and Seely, 1979; Ingersol1, 1979; Bottjer and Link, 1984). The Cenomanian–Eocene forearc strata that are the focus of this study occur in a NNW-to-SSE–oriented outcrop belt from southern Oregon to Baja California (Fig. 2A). Sampled stratigraphic units are from several forearc depocenters that have unique structural and stratigraphic histories (see Appendix DR3 for additional geologic background on individual forearc depocenters[1]).

The Great Valley and Peninsular Ranges segments of the forearc are well preserved, and both extend for hundreds of kilometers along the margin (Kennedy and Moore, 1971; Ingersoll, 1979; Bottjer and Link, 1984). Both forearc segments onlap the western margin of the Sierran–Peninsular Ranges arc and are inferred to have been confined to the west by an actively accreting subduction complex (Dickinson, 1995a; Williams and Graham, 2013). Upper Cretaceous–Eocene forearc strata of the Salinian block and Transverse Ranges are widespread in the California Coast Ranges (Graham, 1976a, 1976b; Grove, 1993; Dickinson, 1995b), where Neogene deformation associated with the development of the modern strike-slip plate boundary has obscured pre-Neogene geologic relationships (Atwater, 1989). Forearc strata in these regions were deposited atop deeply denuded plutonic rocks of the mid-Cretaceous batholithic belt or Franciscan subduction complex (Dickinson, 1995b; Kidder et al., 2003).

Palinspastic Reconstruction

The original distribution of Upper Cretaceous–Eocene forearc strata has been greatly modified by deformation associated with the development of the San Andreas plate boundary (Atwater, 1989), including large-magnitude offset along strike-slip faults (Hill and Dibblee,

[1]GSA Data Repository item 2014263, data sources used in Figure 2, explanation of the palinspastic reconstruction, sample location descriptions, plots of cumulative detrital zircon U-Pb age distributions, and data tables, is available at http://www.geosociety.org/pubs/ft2014.htm or by request to editing@geosociety.org.

1953; Graham et al., 1989; Dickinson et al., 2005) and microplate capture and associated transrotation of crustal blocks in the western Transverse Ranges and southern California continental borderland (Luyendyk, 1991; Nicholson et al., 1994; Dickinson, 1996). Additional disruption has occurred by (1) backarc extension within the Basin and Range Province (Wernicke, 1992), (2) local domain rotation within the Mojave Desert region (Dickinson, 1996), (3) inboard dextral offset (e.g., the Eastern California shear zone; Dokka and Travis, 1990), and (4) local compressional and extensional tectonism in the California Coast Ranges (Crowell, 2003).

We present a generalized palinspastic reconstruction that integrates previous interpretations (Grove et al., 2003a; Dickinson et al., 2005; Jacobson et al., 2011) with updated fault offset estimates (Graymer et al., 2002; Sharman et al., 2013) in an effort to restore original paleogeologic relationships that existed along the California continental margin during Eocene time (Fig. 2B). In general, our reconstruction follows that of Graymer et al. (2002) for the San Franciscan Bay region, Dickinson et al. (2005) for the Salinian block, and Jacobson et al. (2011) for the Transverse Ranges and Peninsular Ranges (see Appendix DR2 for additional details [see footnote 1]). We do not attempt to restore slip on the Nacimiento fault, given its controversial and uncertain structural history (e.g., Dickinson et al., 2005; Ducea et al., 2009). Because the Nacimiento fault is thought to have been active from latest Cretaceous to Paleocene time (ca. 75–60 Ma; Jacobson et al., 2011), offset along this structure likely influenced the relative positions of Cenomanian–Paleocene forearc strata along the margin as depicted in Figure 2B.

A major difference between our palinspastic reconstruction and those of previous workers is the addition of ~100 ± 25 km of offset (Sharman et al., 2013) to the commonly quoted ~315 km (e.g., Graham, 1978; Graham et al., 1989) along the central San Andreas fault that restores the Salinian block to an intra-Cordilleran arc position (Fig. 2B). This reconstruction differs from models that depict the northern Salinian block as being juxtaposed against the outboard edge of the forearc and subduction complex of the southern San Joaquin basin during Paleogene time (e.g., Nilsen and Clarke, 1975; Hall, 1991; Hall and Saleeby, 2013). Our palinspastic reconstruction is consistent with regional provenance trends that suggest the northern Salinian block was juxtaposed against the southernmost Sierra Nevada in middle Eocene time (Sharman et al., 2013), and alignment of the northern extent of the Salinian block (Navarro structural discontinuity) with the inferred western edge of Sierran basement beneath the fill of the San Joaquin basin (Dickinson et al., 2005). Because the displaced Pinnacles and Neenach volcanic centers (ca. 23 Ma) are offset by only ~315 km (Matthews, 1976), our restoration implies that this additional displacement must have occurred between middle Eocene and early Miocene time (ca. 38–23 Ma; Sharman et al., 2013). Alternatively, portions of the additional ~100 ± 25 km slip could be accounted for by lengthening (or “telescoping”) the Salinian block via internal strike-slip faulting or compression (e.g., routing Reliz-Rinconada fault displacement into the northern Salinian block; Dickinson et al., 2005, their fig. 10) or by back-rotating the southernmost Sierra Nevada (Kanter and McWilliams, 1982), thereby shifting the northern Salinian block southward (Dickinson, 1996).

Our restoration of the Salinian block results in the total displacement on the central San Andreas fault being greater than estimates for the cumulative displacement along the San Andreas fault system in southern California (~415 km vs. ~325 km), including offset along the Canton fault, San Gabriel fault, and various strands of the San Andreas fault (Crowell, 2003). We account for this discrepancy by routing excess slip through the western Transverse Ranges to a fault located offshore peninsular California. A potential candidate for this structure is the San Benito–Tosco–Abreojos fault, which is known to have accommodated right-lateral offset between the Pacific and Northern American plates between ca. 12 and 5 Ma and prior to inland migration of the transform boundary to initiate the opening of the Gulf of California (Spencer and Normark, 1979; Dickinson, 1996). During this time period, the central San Andreas fault must have been linked with the San Benito–Tosco–Abreojos fault by a fault, or series of faults, that ran through what is today the western Transverse Ranges and California continental borderland. Unfortunately, any structures that accommodated pre–middle Miocene slip have been strongly overprinted by transrotation (Luyendyk, 1991; Dickinson, 1996) and local transpression in Pliocene–Holocene time (Crowell, 2003).

METHODS AND DATA SOURCES

Detrital Zircon U-Pb Ages

This study presents a compilation of U-Pb crystallization ages of detrital zircons from Upper Cretaceous–Eocene forearc sandstone from California and areas immediately to the north (southern Oregon) and south (northern Baja California; Fig. 2). In total, this data set includes more than 12,000 detrital zircon U-Pb ages from more than 200 sandstone samples, of which 4474 grains from 66 samples are fully published herein for the first time. The GSA Data Repository (see footnote 1) contains a complete list of samples used in this study (Table DR1), analytical results (Tables DR2–DR5), and a description of sample locations (Appendix DR3). We also present a comparison of forearc strata with time-equivalent units in the Franciscan subduction complex (681 grains from 10 samples), underplated Upper Cretaceous–Lower Paleogene schist (2027 grains from more than 60 samples), and strata from intra-arc and retroarc positions (2550 grains from 31 samples; see Table DR1 for data sources [see footnote 1]).

Because this data set contains samples collected and analyzed by different authors for different purposes, the number of grains analyzed per sample varies widely (9–178 grains), with the median sample having ~56 grains (Table DR1 [see footnote 1]). Most studies analyzed either ~100 or ~60 randomly selected grains per sample following typical sampling procedures for detrital zircon provenance studies (e.g., Dickinson and Gehrels, 2009). However, much of the data set from the Salinian block, Transverse Ranges, and Peninsular Ranges was collected to maximize sample coverage at the expense of the number of grains per sample analyzed (e.g., Jacobson et al., 2011). In these regions, the median sample has ~30 grains analyzed.

All zircon grains presented herein were analyzed using either secondary ionization mass spectrometry (SIMS) or laser-ablation–inductively coupled plasma–mass spectrometry (LA-ICP-MS). Data sets acquired using LA-ICP-MS tend to have more grains analyzed per sample than those acquired using SIMS due to the relative ease of collecting large data sets using the former method. Zircon grain ages collected as part of this study were analyzed using (1) a multicollector LA-ICP-MS at the University of Arizona (for a description of methods, see Gehrels et al., 2008; Cassel et al., 2012), (2) a single-collector LA-ICP-MS at the University of California–Santa Cruz (Sharman et al., 2013), and (3) a SIMS Cameca IMS 1270 ion microprobe at the University of California–Los Angeles (Grove et al., 2003a).

We combined individual samples into groups based upon both reconstructed paleogeography and depositional age to emphasize major provenance trends at the expense of local variability and to facilitate presentation of data (e.g., LaMaskin, 2012). Sample groups were further combined to form six regional groups that reflect basin configuration and reconstructed north-south position along the forearc: (1) Oregon forearc (including the Tyee and Hornbrook basins), (2–3) Great Valley forearc (subdivided into the Sacramento and San Joaquin basins), (4) northern and central Salinian block (hereafter "Salinian block forearc"), (5) southern Salinian block and Transverse Ranges (hereafter "Transverse Ranges forearc"), and (6) Peninsular Ranges forearc (Table DR1 [see footnote 1]). These regional groups are defined with the purpose of emphasizing major provenance transitions along the margin.

In addition to defining geographic groupings, we divided the data set into four additional depositional age categories: (1) Cenomanian to Coniacian, (2) Santonian to Campanian, (3) Maastrichtian to Paleocene, and (4) early to middle Eocene (Table DR1 [see footnote 1]). These age divisions were chosen based on periods of major reorganization within the forearc. For example, the Coniacian-Santonian boundary approximately coincides with major changes in both sandstone petrology and detrital zircon age populations in the Great Valley forearc (Ingersoll, 1983; DeGraaff-Surpless et al., 2002). The Campanian-Maastrichtian boundary approximately corresponds with a shift to inboard provenance in the Salinian block and Transverse Ranges (Jacobson et al., 2011). Because displaying results from individual samples is precluded by the large number of samples in the data set, we provide cumulative U-Pb age distributions from individual samples within each location and age group as Appendix DR4 (see footnote 1).

RESULTS

Detrital Zircon Geochronology

A compilation of normalized and cumulative detrital zircon U-Pb age distributions is presented in Figure 3 for Upper Cretaceous–Eocene forearc sandstone samples by location and age. Although the majority of zircon grains are Mesozoic in age, wide ranges of age populations are present that indicate derivation from both local and extraregional source regions (Table 1; DeGraaff-Surpless et al., 2002; Jacobson et al., 2011; Sharman et al., 2013). In general, detrital zircon grains can be divided, from most to least abundant, into three first-order age populations (Table 1): (1) Late Permian–Cretaceous Cordilleran arc zircon assemblages (ca. 285–65 Ma), (2) pre-arc Paleozoic and Precambrian assemblages (older than ca. 285 Ma), and (3) Paleogene zircon assemblages (ca. 65–40 Ma). Arc-derived detrital zircons can be divided into subpopulations that reflect episodic magmatism in the Cordilleran arc (Fig. 4). Major magmatic pulses in the Sierra Nevada, Salinian block, Mojave Desert region, and Peninsular Ranges occurred during Permian–Triassic time (ca. 285–225, peak at ca. 252 Ma), Middle–Late Jurassic time (ca. 180–135 Ma, peaks at ca. 162–148 Ma), and mid-Cretaceous time (ca. 125–80 Ma, peak at ca. 97 Ma) (Fig. 4). Less pronounced but still distinct pulses occurred at ca. 77 Ma and ca. 49 Ma (Fig. 4). The peaks of age populations observed in the detrital record correspond closely with those from exposed volcanic and plutonic rocks (Fig. 4).

Figures 5 and 6 display cumulative and normalized age distributions of regional (basin-scale) groups, and Figure 7 illustrates the spatial and temporal (Cenomanian–Eocene) evolution of major detrital zircon age populations along ~2000 km of the margin from southern Oregon to northern Baja California. Cenomanian–Campanian forearc strata (3989 grains from 79 samples) tend to be dominated by Jurassic to mid-Cretaceous (ca. 200–85 Ma) zircon (45%–100%; median 93%; Figs. 3A, 3B, and 5–7; Table DR6 [see footnote 1]). In particular, Jurassic–earliest Cretaceous (200–135 Ma) zircon forms a significant component of Great Valley forearc strata but dramatically decreases in abundance southward (Figs. 3A, 3B, and 7). Late Permian–Triassic zircon is uncommon (0%–7%), and pre–300 Ma zircon is generally rare (0%–48%, median 3%) but constitutes an important component of some Santonian–Campanian sandstone samples (e.g., Del Puerto Canyon, Chico, and Cache Creek; Fig. 3B). Strata from the Peninsular Ranges forearc are characterized by nearly unimodal distributions with peaks at ca. 110–95 Ma that are only slightly older than the depositional ages of these samples (Figs. 3A and 3B).

Maastrichtian–Paleocene forearc strata (1652 grains from 41 samples) display a comparatively wider range of detrital zircon age distributions than their Cenomanian–Campanian counterparts (Figs. 3C and 7). Although strata deposited within the Great Valley forearc are still dominated by Jurassic to mid-Cretaceous (200–85 Ma) zircon (87%–98%, median 93%), these samples display higher proportions of 100–85 Ma zircon (8%–56%, median 32%) than their Cenomanian–Campanian counterparts (0%–33%, median 2%; Fig. 7). Maastrichtian–Paleocene forearc strata in the Transverse Ranges and Santa Ana Mountains are characterized by higher abundances of latest Cretaceous (85–65 Ma) zircon (0%–89%, median 21%) and pre-arc detrital zircon (0%–92%, median 40%) than time-equivalent strata to the north (Figs. 3C and 7). Samples from San Miguel Island, the San Diego area, and El Rosario area are dominated by mid-Cretaceous zircon (79%–96%; Figs. 3C and 7).

Wide ranges of detrital zircon age populations are present in early to middle Eocene forearc strata (6479 grains from 89 samples; Fig. 3D). Mid-Cretaceous zircon (ca. 135–85 Ma) is abundant in the Great Valley forearc (19%–94%, median 74%) but decreases in abundance in the northern and central Salinian block (2%–87%, median 35%) and in the Transverse Ranges and northern Santa Ana Mountains (0%–25%, median 7%; Figs. 3D and 7). Jurassic zircon becomes a dominant constituent in the northern and central Salinian block (12%–92%, median 42%) relative to older forearc counterparts (Figs. 3D and 7). The Transverse Ranges and adjacent northern Peninsular Ranges forearc contain abundant latest Cretaceous (0%–42%, median 17%) and pre-arc zircon (27%–75%, median 57%; Figs. 3D and 7).

SEDIMENTARY PROVENANCE ANALYSIS

The following sections provide a discussion of the potential source regions that we interpret to have been capable of producing the zircon age populations present in the California forearc (Table 1).

Pre-Permian (Older than Ca. 300 Ma) Zircon

Pre-Permian (i.e., pre–Cordilleran arc) zircon can be divided into a variety of subpopulations that range from Paleozoic to Archean in age and reflect derivation from a variety of ultimate sources in Laurentia (Table 1; Dickinson and Gehrels, 2009; Dickinson et al., 2012). Although some pre–300 Ma age populations could have been derived from the local Proterozoic framework of the southwestern United States (e.g., late Paleoproterozoic Yavapai-Mazatzal Province), some exotic age populations (e.g., Grenville Mesoproterozoic) have no local bedrock source and likely were originally derived from the Appalachian orogen and transported across the continent via fluvial and eolian processes to the Cordilleran miogeocline and retroarc foreland (Dickinson and Gehrels, 2009).

Pre-arc detrital zircon in forearc sandstone can be divided in two general assemblages (Jacobson et al., 2011). The first is characterized by a wide spread of age peaks that span Paleozoic to Archean ages and is found in Cenomanian–Campanian strata along the entire California margin and in Maastrichtian–Eocene strata of the Great Valley forearc (Fig. 3). Although this age assemblage could be derived from a large number of sources in the western United States (see previous), the most likely source for these pre–300 Ma zircon grains is recycling from wall rocks of the Cordilleran Mesozoic arc (Grove et al., 2008; Jacobson et al., 2011) or from

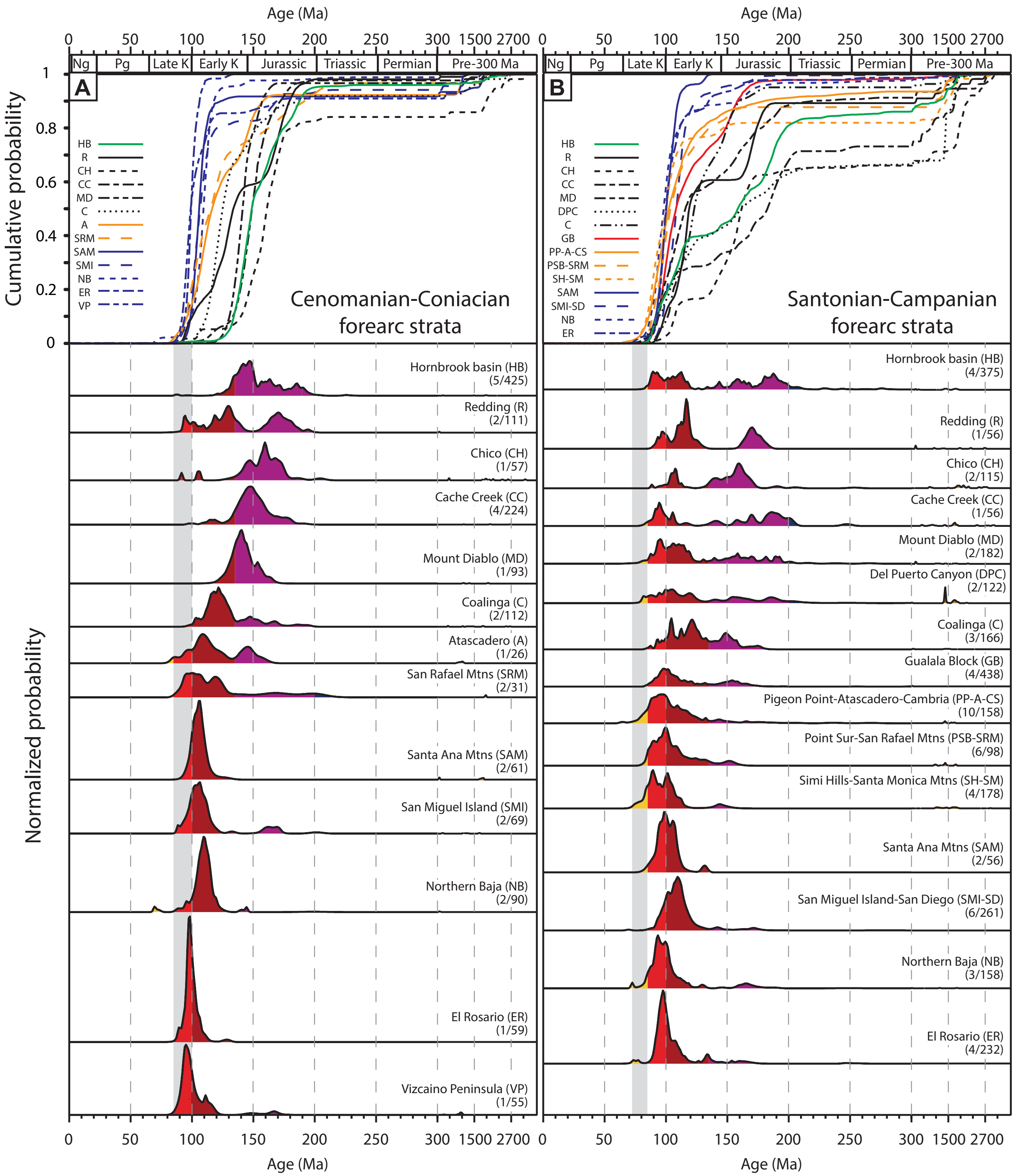

Figure 3 (*on this and following page*)**. Cumulative and normalized distributions of detrital zircon U-Pb ages for groups of Upper Cretaceous–Eocene forearc strata. Cumulative distributions are colored according to regional group (green—Oregon forearc; black—Great Valley forearc; red—Salinian forearc; yellow—Transverse Ranges forearc; blue—Peninsular Ranges forearc). Number of samples/grains shown in parentheses. The vertical scale of normalized distributions greater than 300 Ma are displayed at 1/10th scale. See Table DR1 for additional information on sample groups and data sources (text footnote 1). Ng—Neogene, Pg—Paleogene, K—Cretaceous.**

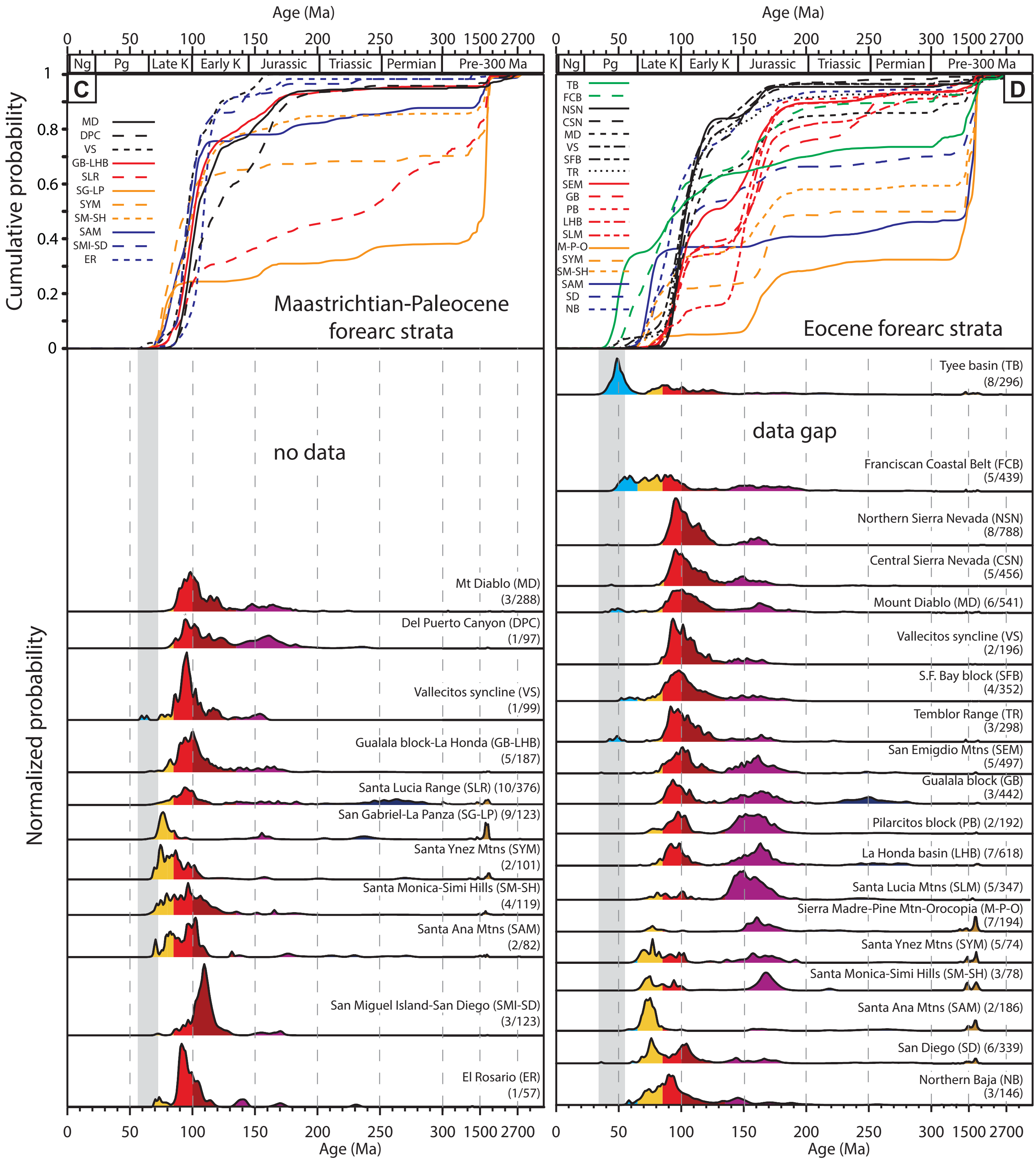

Figure 3 (*continued*).

TABLE 1. DETRITAL ZIRCON U-Pb AGE POPULATIONS

Age population	Approx. age range (Ma)	Peak age(s) (Ma)	Inferred source region(s)
I. Paleogene grains			
Ia. Early to middle Eocene	43–52	ca. 50	Challis volcanic center
Ib. Paleocene to early Eocene	53–65	N.A.	Idaho batholith
II. Cretaceous–Permian grains			
IIa. Late Cretaceous	65–85	N.A.	Idaho batholith or "Laramide-aged" plutons in southwest United States
IIb. Mid- to Late Cretaceous	80–125	ca. 97	Idaho batholith (<98 Ma) or mid-Cretaceous Cordilleran arc
Magmatic gap	125–135	N.A.	
IIc. Jurassic to earliest Cretaceous	135–180	ca. 148–162	Jurassic Cordilleran arc or accreted Jurassic oceanic-island arcs
Magmatic gap	180–225	N.A.	
IId. Late Permian–Triassic	225–285	ca. 252	Late Permian–Triassic Cordilleran arc
III. Pre-Permian grains*			
IIIa. Paleozoic to Neoproterozoic grains	300–700	N.A.	Appalachian orogen, accreted Paleozoic terranes, and rift plutons
IIIb. Grenville Mesoproterozoic	912–1310	N.A.	Grenville Province (eastern-southern Laurentia)
IIIc. Pre-Grenville Mesoproterozoic	1311–1579	N.A.	Anorogenic granitic plutons (southwest Laurentia)
IIId. Late Paleoproterozoic	1581–1855	N.A.	Yavapai-Mazatzal Province (southwest Laurentia)
IIIe. Older Paleoproterozoic	1855–2430	N.A.	Multiple northern Laurentian-age provinces
IIIf. Archean	2470–3058	N.A.	Superior Province of northeast Laurentia

*Pre-Permian grain age populations modified from Dickinson et al. (2012)

accreted Paleozoic terranes located outboard of the mid-Cretaceous arc in northern California (Figs. 2 and 3; DeGraaff-Surpless et al., 2002; Surpless and Beverly, 2013). This interpretation is supported by the overwhelming abundance of arc-derived zircon present in these samples (Figs. 3, 6, and 7; Jacobson et al., 2011).

The second pre-arc age assemblage is found in Maastrichtian–Eocene forearc strata of the Transverse Ranges and Peninsular Ranges and is characterized by a major peak at ca. 1700 Ma, a secondary peak at ca. 1400 Ma, and a conspicuous absence of Paleozoic–Neoproterozoic zircon and zircon older than ca. 1850 Ma (Fig. 3). This assemblage was likely derived from first-cycle erosion of late Paleoproterozoic–Mesoproterozoic crystalline rocks of the Mojave Desert region and the Mogollon highlands of southwestern Arizona (Fig. 2; Jacobson et al., 2011; Dickinson et al., 2012). Comparison with Upper Cretaceous and Paleogene strata deposited on the flanks of the Arizona Mogollon highlands reveals nearly identical age peaks and proportions (Dickinson and Gehrels, 2008; Dickinson et al., 2012). This assemblage also frequently occurs in conjunction with latest Cretaceous (85–65 Ma) zircon (Figs. 3C, 3D, and 7), and igneous rocks of this age are present in the eastern Mojave Desert and Mogollon highlands regions (Fig. 2).

Permian–Triassic (Ca. 285–225 Ma) Zircon

Late Permian and Triassic volcanic and plutonic rocks are relatively uncommon in California but are locally present in the eastern Sierra Nevada, Mojave Desert, and Transverse Ranges (Fig. 4; Dilles and Wright, 1988; Walker et al., 2002; Barth and Wooden, 2006). Here, the Permian–Triassic volcanic arc lies inboard of the mid-Cretaceous arc in approximately the same position as the continental Jurassic arc (Fig. 2). Permian to Triassic rocks are also present in the Mexican segment of the Cordilleran arc and in the accreted Guerrero superterrane (Dickinson and Lawton, 2001; Centeno-García et al., 2008), although the relative paucity of 300–200 Ma zircon in the Transverse Ranges and Peninsular Ranges forearc suggests that Mexican Permian–Triassic rocks were not a significant source to the continental margin at this latitude (Kimbrough et al., 2014a).

Jurassic to Earliest Cretaceous (Ca. 180–135 Ma) Zircon

Arc-related volcanic and plutonic rocks of Jurassic and earliest Cretaceous age are widespread along the California continental margin and in the southwestern United States in general (Figs. 2 and 4; Irwin and Wooden, 2001; Barton et al., 2011). The present-day distribution of Jurassic rocks is generally divided into regions outboard and inboard of the mid-Cretaceous arc (Klamath Mountains and northern Sierra Nevada, and southeastern Sierra Nevada, Mojave Desert, and Sonoran Desert, respectively; Fig. 2). In addition, Jurassic to earliest Cretaceous island arcs of the Guerrero superterrane are present in Baja California (Dickinson and Lawton, 2001; Centeno-García et al., 2008), and Jurassic gneissic granites are present within the central Peninsular Ranges (Shaw et al., 2003). Together, these rocks are capable of providing a local source of the scarce 180–135 Ma zircon that is found in the Peninsular Ranges forearc (Fig. 7; Dickinson and Lawton, 2001; Shaw et al., 2003). These sources may have also provided Jurassic zircon to Upper Jurassic forearc strata (Peñasquitos Formation) prior to the development of the mid-Cretaceous Peninsular Ranges arc (Kimbrough et al., 2014a). A "magmatic lull" (ca. 135–125 Ma) separates Jurassic–earliest Cretaceous from mid-Cretaceous arc volcanism (Fig. 4; Barton et al., 2011). This gap is also clearly reflected in the detrital record (Fig. 4), although zircon grains in this age range constitute an important age population in some forearc sandstone samples (e.g., Cenomanian–Campanian Great Valley forearc; DeGraaff-Surpless et al., 2002; Figs. 3A and 3B).

Mid-Cretaceous (Ca. 125–85 Ma) Zircon

Volcanic and plutonic rocks of the mid-Cretaceous Cordilleran arc are widespread along the margin as a result of voluminous arc

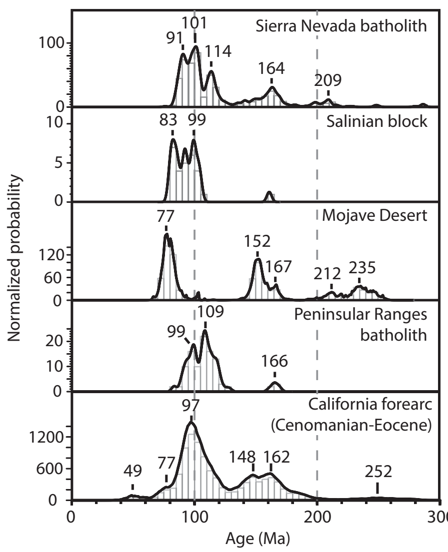

Figure 4. Zircon U-Pb age distributions (≤300 Ma) for volcanic and plutonic rocks from the Sierra Nevada batholith, Salinian block, Mojave Desert region, and Peninsular Ranges batholith (Premo et al., 1998; Silver and Chappell, 1988; Grove et al., 2008; Chapman et al., 2012; Barth et al., 2013; Kimbrough et al., 2014b) and Cenomanian–Eocene forearc strata (see Table DR1 for data sources [text footnote 1]).

magmatism and batholithic emplacement from Idaho to Baja California (Figs. 1 and 2; Chen and Moore, 1982; Cowan and Bruhn, 1992; Todd et al., 2003). In particular, mid- to Late Cretaceous arc rocks comprise the majority of the Sierra Nevada batholith, Salinian block, and Peninsular Ranges batholith and are common in the Transverse Ranges and Mojave Desert region (Figs. 2 and 4; Irwin and Wooden, 2001; Kistler and Champion, 2001; Walker et al., 2002; Todd et al., 2003). We further subdivide this age population into pre– and post–100 Ma divisions to reflect an eastward migration of magmatism over time that is recorded in the Sierran–Peninsular Ranges arc (Fig. 2; Chen and Moore, 1982).

Latest Cretaceous (85–65 Ma) Zircon

Magmatism in the Sierran–Peninsular Ranges segments of the Cordilleran arc ended by ca. 85–80 Ma as a result of the onset of Laramide flat-slab subduction (Chen and Moore, 1982; Irwin and Wooden, 2001). However, plutonic rocks of latest Cretaceous (ca. 85–65 Ma) age are widespread inboard of the mid-Cretaceous arc in southeastern California, southwestern Arizona, and Sonora Mexico (Figs. 2 and 4; Lipman, 1992; Barth et al., 1995; McDowell et al., 2001; Wells and Hoisch, 2008). These rocks are likely the source of the latest Cretaceous zircon found in Maastrichtian–Eocene strata of the Transverse Ranges and Peninsular Ranges forearc (Fig. 3; Jacobson et al., 2011). This age range also overlaps with the Idaho batholith (ca. 95–53 Ma; Gaschnig et al., 2011). The association of latest Cretaceous and Paleogene zircon in the Eocene Tyee basin and Great Valley forearc (Fig. 3D) suggests a distant origin in central Idaho for these grains (Dumitru et al., 2012).

Paleogene (Ca. 65–40 Ma) Zircon

A local source of the Paleogene zircon found in some forearc sandstone samples (Fig. 3D) is unlikely because there are no known sources of volcanic or plutonic rocks of this age in California (Fig. 2). However, early Cenozoic igneous rocks are widespread in the interior of the western United States (Lipman, 1992). Dumitru et al. (2012) established that detritus of this age reached the continental margin via rivers that drained the Idaho batholith (98–53 Ma; Gaschnig et al., 2011) and the Challis volcanic field (51–43 Ma; M'Gonigle and Dalrymple, 1996; Chetel et al., 2011; Gaschnig et al., 2011) in Eocene time. Eocene–Oligocene zircon (ca. 44–29 Ma) is also present in western flowing drainages in the northern Sierra Nevada that were likely sourced from volcanic rocks in

Figure 5. Cumulative distributions of detrital zircon U-Pb ages (≤200 Ma) for regional groups of Late Cretaceous–Eocene forearc strata (see Table DR1 for additional information on sample groups and data sources [text footnote 1]). Thick, gray lines are zircon U-Pb age distributions from plutonic and igneous rocks from the Sierra Nevada batholith, Salinian block, Mojave Desert region, and Peninsular Ranges batholith (see data sources in Fig. 4). Abbreviations: Cen—Cenomanian; Cmp—Campanian; Con—Coniacian; Eoc—Eocene; Ma—Maastrichtian; MD—Mojave Desert; Pc—Paleocene; PRB—Peninsular Ranges batholith; San—Santonian; SB—Salinian block; SNB—Sierra Nevada batholith.

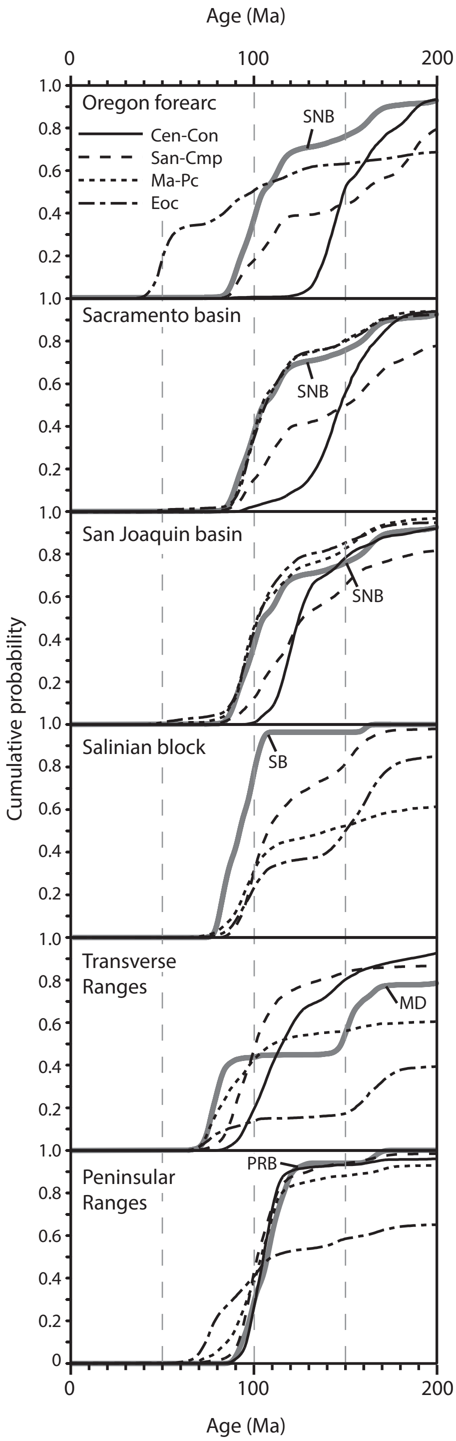

northern Nevada (Cassel et al., 2012). However, most of the samples that contain this young age population are late Eocene or Oligocene in age, based on the youngest zircon grains and stratigraphic relationships (Cassel et al., 2012). Furthermore, fluvial samples thought to be as old as middle Eocene in age lack zircon younger than ca. 90–80 Ma (with a single exception of a 41.5 Ma grain in sample CEC-5; Cecil et al., 2010; Cassel et al., 2012). This suggests that Sierran fluvial drainages were not a significant source of Nevadan Paleogene zircon to the Great Valley forearc until late Eocene time. For these reasons, the central Idaho region is most likely to have been the source of Paleogene zircon to the early–middle Eocene Great Valley forearc, associated trench-slope basins, and the subduction complex.

Igneous rocks as young as 50 Ma are also present in southwestern Arizona and Sonora, Mexico (Jacobson et al., 2011). These sources likely account for the few Eocene grains found in the Poway fluvial system in northern Baja but otherwise were not a significant source to other Paleogene forearc strata in southern California.

DISCUSSION

Temporal and Spatial Evolution of Forearc Provenance and Paleogeography

Figure 8 presents a generalized depiction of the paleogeographic evolution of the Cordilleran margin from Late Cretaceous to middle Eocene time based upon observed spatial and temporal trends in forearc detrital zircon age signatures (Fig. 7). We also compared forearc age distributions with those from contemporaneous strata in intra-arc and retroarc positions (e.g., Barth et al., 2004; Dickinson and Gehrels, 2008; Dickinson et al., 2012; Fig. 6). The restored north-to-south positions of forearc strata (Figs. 7 and 8) are inferred from our palinspastic reconstruction of the margin (Fig. 2B) and are thus subject to uncertainties inherent in such reconstructions (see Appendix DR2 [see footnote 1]). In particular, the structural history of the Nacimiento fault has important implications for pre-Eocene forearc relationships (e.g., Jacobson et al., 2011). Even so, this compilation reveals systematic, margin-scale provenance trends in the California forearc that reflect the tectonic and landscape evolution of the continental margin (Figs. 7 and 8).

Cenomanian–Coniacian Forearc (100–86 Ma)

Although Cenomanian–Coniacian forearc strata are dominated by Jurassic to mid-Cretaceous (200–85 Ma; 83%–100%) zircon, the contributions from various arc subpopulations vary systematically along the forearc, with peak detrital zircon ages becoming progressively younger toward the south (Figs. 3A and 7). Jurassic–earliest Cretaceous (200–135 Ma) zircon grains constitute a majority of the forearc sandstone samples in the Hornbrook and Sacramento basins (41%–100%), with samples from Cache Creek and Mount Diablo displaying nearly unimodal age distributions with peaks at ca. 148 and 140 Ma, respectively (Fig. 3A). The abundance of 200–135 Ma zircon in this region clearly reflects the presence of accreted Triassic–Jurassic assemblages (Klamath Mountains and Foothills belt) that occur outboard of the mid-Cretaceous arc at these latitudes (~43–37°N; Figs. 1 and 2). These forearc strata also display a conspicuous scarcity of contemporary (100–86 Ma) zircon despite concurrent emplacement of the voluminous Sierra Crest intrusive suite in the adjacent Sierra Nevada arc (Chen and Moore, 1982; Coleman and Glazner, 1997; Ducea, 2001; see following discussion).

Forearc strata south of the Sacramento basin display a systematic shift toward younger, mid-Cretaceous (125–85 Ma) ages that suggests decreased contribution from outboard Triassic–Jurassic assemblages and increased contribution from the mid-Cretaceous arc (Fig. 7). In particular, Jurassic–earliest Cretaceous (200–135 Ma) zircon becomes scarce in the Peninsular Ranges forearc (0%–14%; Fig. 7). This observation suggests that any contribution from Jurassic rocks within the Peninsular Ranges or from the Guerrero superterrane was overwhelmed by the voluminous mid- to Late Cretaceous batholith and its volcanic equivalents. Although 100–85 Ma zircon is nearly absent in the Great Valley forearc, this population becomes increasingly abundant toward the south (Fig. 7). The presence of post–100 Ma zircon in the Peninsular Ranges forearc suggests that the eastern batholith (La Posta suite; Walawender et al., 1990) was a source to the forearc during this time period (Fig. 7). In particular, Cenomanian to Turonian strata in the El Rosario area and Vizcaino Peninsula are highly enriched in post–100 Ma zircon relative to samples to the north (Fig. 3A; Kimbrough et al., 2001).

Figure 6 (*on following page*). Cumulative and normalized distributions of detrital zircon U-Pb ages for arc-derived detrital zircon (i.e., ≤300 Ma) from groups of forearc, subduction complex, underplated schist, intra-arc, and retroarc strata (see Table DR1 for samples and data sources [see text footnote 1]). Numbers in parentheses indicate the number of samples/grains younger than 300 Ma and the percentage of this subpopulation relative to the total population. Abbreviations: Cum—cumulative; FC—Franciscan Complex; MRA—McCoy retroarc, OR—Oregon, PR—Peninsular Ranges, Prob—probability, RAF—retroarc foreland, SB—Salinian block, SC—Sacramento basin, SCH—underplated schist, SJ—San Joaquin basin, TR—Transverse Ranges.

We interpret the dominance of arc-derived (ca. 200–85 Ma) zircon in Cenomanian–Coniacian forearc strata (Fig. 7) to suggest that the forearc was completely isolated from inboard source areas and that the mid-Cretaceous arc formed a continuous, high-standing topographic feature (Fig. 8A). The scarcity of post–100 Ma zircon indicates little derivation from the eastern portion of the mid-Cretaceous arc, except along the southernmost portion of the study area (Figs. 2 and 7). In addition, age-equivalent retroarc strata are enriched in post–100 Ma zircon relative to the forearc and also contain abundant Triassic–Jurassic zircon that suggests derivation from older segments of the Cordilleran arc that occur inboard of the mid-Cretaceous arc (Figs. 2 and 6). Correspondingly, a drainage divide is inferred to have existed along the axis of the Cretaceous arc, which we depict along the western rim of the elevated Nevadaplano to the north and west of the retroarc McCoy Mountains basin in the south (Barth et al., 2004; Spencer et al., 2011; Fig. 8A). The scarcity of arc-derived zircon (3%–5%; Dickinson et al., 2012, their Fig. 5) in the foreland east of the Sevier thrust front suggests that relatively little arc detritus was able to cross the elevated Nevadaplano to reach the foreland basin to the east.

Santonian–Campanian Forearc (86–72 Ma)

Although Santonian–Campanian forearc strata continue to be dominated by Jurassic to mid-Cretaceous zircon (200–85 Ma; 45%–100%), we observe several distinct changes relative to the older, Cenomanian–Coniacian forearc (Fig. 7). In general, age distributions indicate a decrease in contribution from outboard Triassic–Jurassic assemblages relative to the mid-Cretaceous arc (125–85 Ma; Fig. 7). In particular, widespread influx of 100–85 Ma zircon along the margin signals increased contribution from the eastern, post–100 Ma portion of the mid-Cretaceous arc relative to the pre–100 Ma, western part of the arc (Figs. 2A and 7).

These changes are most clearly observed in the Hornbrook and Sacramento basins, where a dramatic decrease in the abundance of 200–135 Ma zircon corresponds with an abrupt increase in the proportion of 135–85 Ma zircon, particularly the 100–85 Ma subpopulation, at the Coniacian-Santonian boundary (Figs. 3A, 3B, 5, and 7). These samples also contain higher proportions of pre-arc zircon (locally up to 48%, median 15%) relative to their Cenomanian–Coniacian counterparts (up to 16%, median 2%; Fig. 7).

Broadly speaking, the forearc south of the Sacramento basin is characterized by consistent detrital zircon age distributions dominated by mid-Cretaceous (135–85 Ma) zircon (Fig. 7). Peak ages shift toward younger populations and correspondingly are enriched in post–100 Ma zircon relative to their Cenomanian–Coniacian counterparts (Figs. 3A, 3B, 5, and 7). Jurassic–earliest Cretaceous (200–135 Ma) zircon gradually decreases in abundance southward, and strata from San Miguel Island and the San Diego area are enriched in 135–100 Ma zircon relative to others along the margin (Figs. 7 and 8B).

Figure 7 (*on following page*). (A) Spatial distribution of detrital zircon age populations in Cenomanian–Eocene forearc sandstone. Distances are measured north-to-south parallel to the reconstructed Eocene margin (Fig. 2B). Age population abundances are linearly interpolated between sample localities (see Fig. 2A for sample location abbreviations). (B) Inferred spatial and temporal distribution of source regions that supplied detritus to the California forearc (dashed where source contribution is minor or uncertain). Abbreviations: Camp—Campanian; Cen—Cenomanian; Con—Coniacian; HB—Hornbrook basin; Ma—Maastrichtian; Pc—Paleocene; PR—Peninsular Ranges; Sant—Santonian; SB—Salinian block; SCB—Sacramento basin; SJB—San Joaquin basin; TB—Tyee basin; TR—Transverse Ranges.

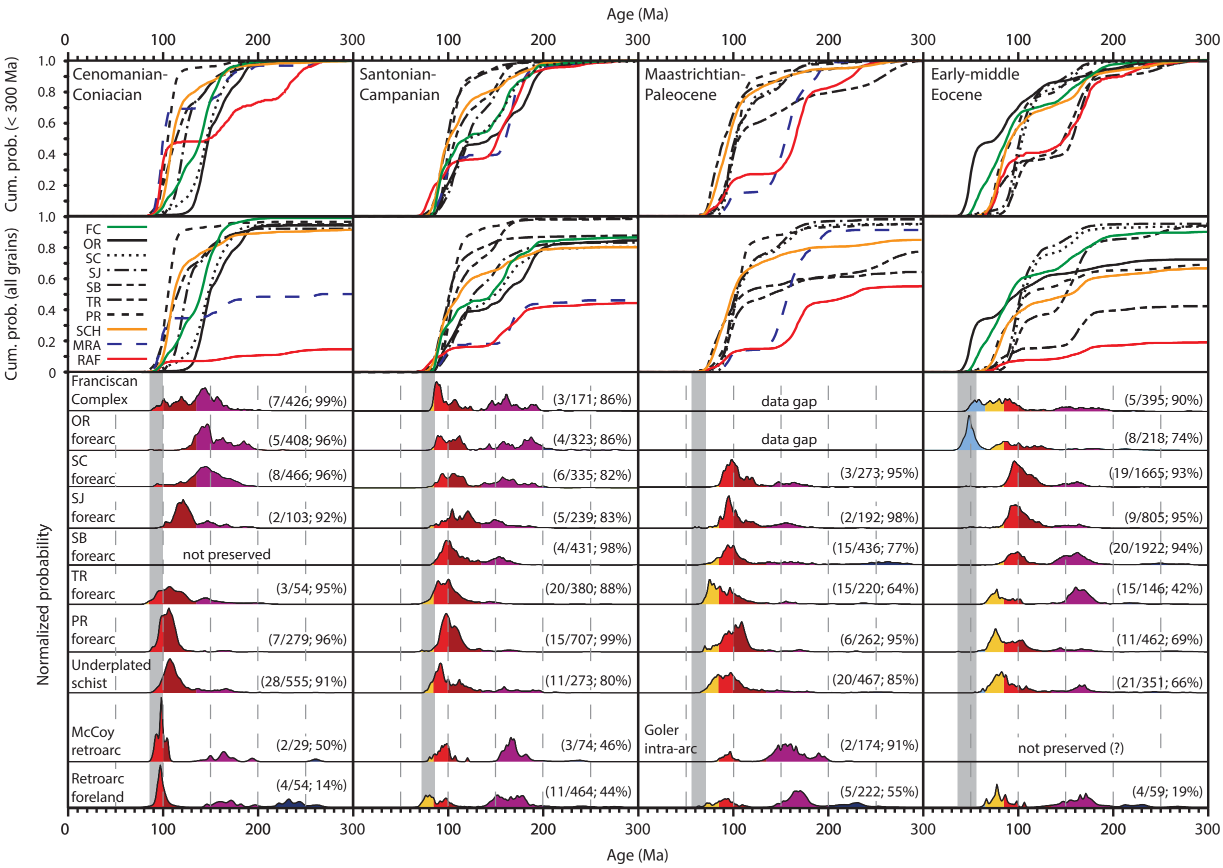

Figure 6.

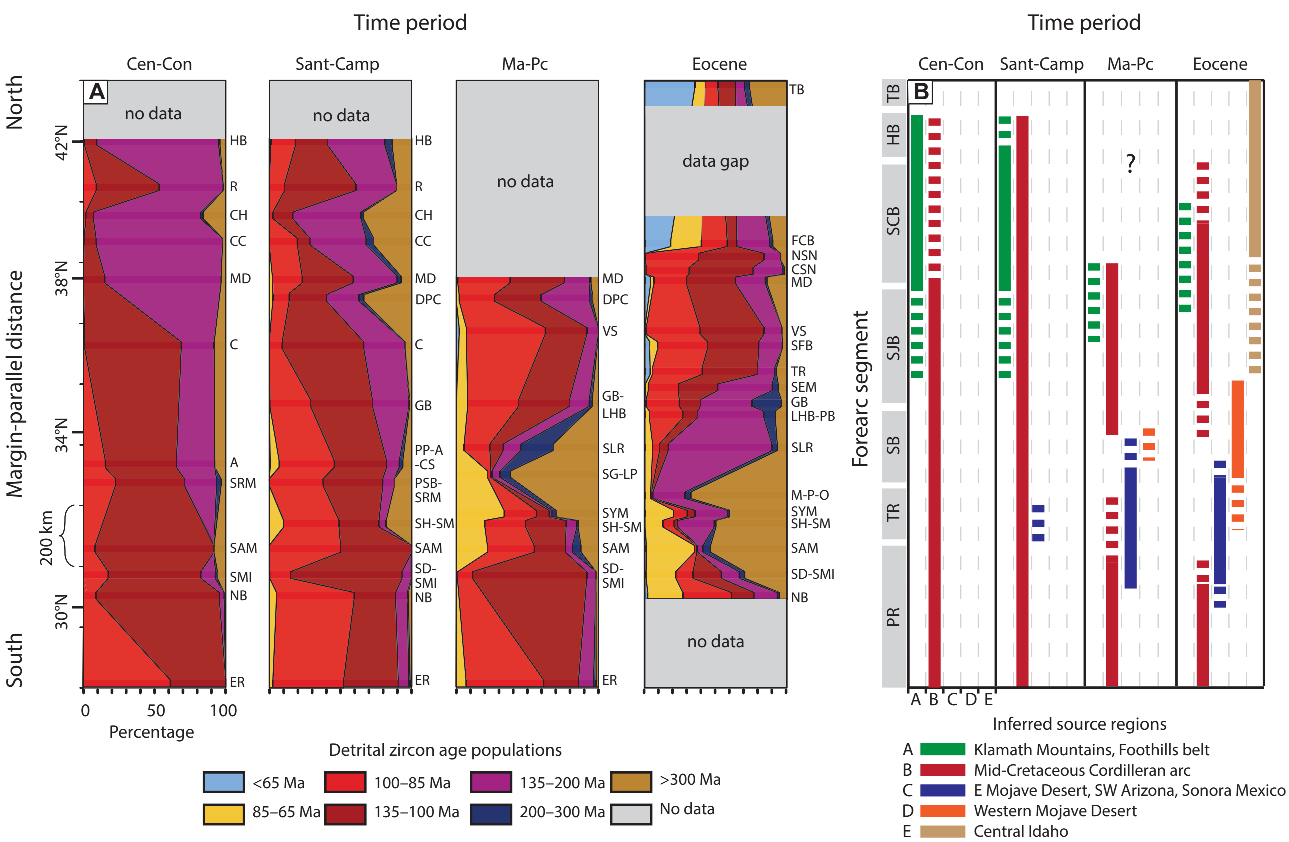

Figure 7.

We infer that increased abundance of 100–85 Ma zircon grains and a widespread shift toward younger peak ages within the forearc basin as a whole signal an eastward migration of drainage divides and progressive unroofing of the mid-Cretaceous batholith immediately following the cessation of arc magmatism (Fig. 8B; see following discussion). Initial dissection of the extinguished Sierran arc at the Coniacian-Santonian boundary is also supported by the transition to the Rumsey petrofacies, which is characterized by an increase in quartz and feldspar and a decrease in lithic fragments and plagioclase-to-total feldspar ratio (Ingersoll, 1983). Increased contribution from the Sierra Nevada batholith to the Great Valley forearc is also supported by an inferred transition from dominantly longitudinal to transverse drainages in this time period (Ingersoll, 1979; DeGraaff-Surpless et al., 2002), coeval with an increase in sedimentation rate and progradation of deltas into the basin (Williams and Graham, 2013).

Detrital zircon age populations in the Santonian–Campanian forearc also indicate continued topographic continuity of the mid-Cretaceous arc and isolation from inboard source regions along most of the margin (Fig. 8B). This inference is supported by comparison with retroarc foreland strata, which contain ca. 85–72 Ma detrital zircons that were sourced from Laramide-aged igneous rocks emplaced inboard of the mid-Cretaceous arc (Figs. 2 and 8B). Age-equivalent forearc strata generally lack zircon younger than ca. 85 Ma, with the exception of late Campanian–early Maastrichtian strata in the Simi Hills and Santa Monica Mountains, which contain a few grains as young as ca. 75 Ma (Figs. 3B, 7, and 8B; Jacobson et al., 2011). Also, Jurassic zircon is abundant in the retroarc but scarce in the forearc (Fig. 6), except in the Hornbrook basin and Great Valley forearc, where Jurassic–earliest Cretaceous zircon was readily supplied from outboard, accreted terranes (Figs. 1 and 2).

Maastrichtian–Paleocene Forearc (72–56 Ma)

Maastrichtian–Paleocene strata in the Great Valley forearc are characterized by a consistent detrital zircon signature that is enriched in 100–85 Ma zircon (25%–56%) relative to their Santonian–Campanian counterparts (0%–23%), suggesting further eastward migration of drainages and continued uplift and denudation of the Sierra Nevada batholith (Figs. 7 and 8C). In addition, lower abundances of Jurassic–earliest Cretaceous (200–135 Ma) zircon suggest diminished input from the Klamath Mountains and accreted terranes in the Sierra Nevada Foothills belt relative to input from the Sierra Nevada batholith (Figs. 7 and 8C). These findings are consistent with studies of sandstone petrology that indicate higher proportions of quartz and feldspar and lower proportions of volcanic lithic grains (Rumsey petrofacies; Ingersoll, 1983). However, although Campanian and Maastrichtian–Paleocene sandstones are petrologically similar arkose, these units are clearly distinguished on the basis of their detrital zircon U-Pb age signatures.

Paleocene strata from the northern Salinian block (Gualala bock and La Honda basin) display provenance signatures that resemble equivalent Great Valley strata in northern exposures. However, Maastrichtian–Paleocene strata from the central Salinian block (Santa Lucia Range) are characterized by a wide range of detrital zircon distributions, including varying proportions of mid-Cretaceous, Jurassic, Permian–Triassic, and Proterozoic age populations (Figs. 3C and 7; see also Appendix DR4 [see footnote 1]). When combined as a group, this region displays detrital zircon age distributions intermediate between those found in the Great Valley forearc and Transverse Ranges (Figs. 7 and 8C). Thus, Maastrichtian–Paleocene strata of the Santa Lucia Range appear to contain a mixed provenance signature that suggests derivation from both local exposures of the mid-Cretaceous batholith and from Triassic–Jurassic igneous rocks in the western Mojave Desert region (Fig. 2).

Forearc strata deposited in the La Panza Range and San Gabriel Mountains exhibit a pronounced switch to source regions inboard of the mid-Cretaceous arc (Figs. 7 and 8C). The abundance of latest Cretaceous (ca. 85–65 Ma) and Proterozoic (ca. 1.8–1.3 Ga) zircon and lack of mid-Cretaceous and Jurassic zircon are consistent with an inland drainage that reached into the eastern Mojave Desert and possibly as far as the Mogollon highlands (Jacobson et al., 2011). The observed influx of inboard detritus is less pronounced in the Santa Ynez Mountains, Simi Hills, and Santa Monica Mountains, where mid-Cretaceous (135–85 Ma) zircon grains still comprise a significant component of the detrital age populations (Fig. 7). The outboard-to-inboard provenance transition in the northern Santa Ana Mountains is recorded as an influx of latest Cretaceous (85–65 Ma) zircon to the Upper Paleocene Silverado Formation (Fig. 7 and 8C). Upper Paleocene–Lower Eocene sandstone from the San Diego area (Mount Soledad Formation) is dominated by ca. 135–100 Ma zircon (81%–96%; Fig. 7), suggesting that these grains were derived locally from the western Peninsular Ranges batholith. However, the presence of Poway porphyritic rhyolite clasts in the Mount Soledad Formation suggests that the drainage at this latitude must have extended inboard to the Sonoran Desert (Kennedy and Moore, 1971; Kies and Abbott, 1982; Abbott and Smith, 1989). We infer that the Jurassic rhyolitic bedrock source of the Poway clasts yielded little sand-sized detritus relative to local batholithic rocks and is thereby underrepresented in the detrital zircon age distributions.

The sudden delivery of abundant inboard detritus to the southern California forearc signals a rapid inland migration of the drainage divide that formerly ran down the axis of the Salinian-Mojave segment of the mid-Cretaceous arc (Jacobson et al., 2011) and was accompanied by marine flooding of the arc interior that extended to at least the San Gabriel block (Figs. 7 and 8C; Kooser, 1982). As a consequence, forearc and retroarc depocenters transitioned from having separate to shared source regions (i.e., Mojave Desert and Mogollon provinces) during this time period (Jacobson et al., 2011; Dickinson et al., 2012; Fig. 6). For example, the Upper Paleocene–Lower Eocene Colton Formation in the Uinta basin is thought to have been supplied via the hypothetical California paleoriver from the Mojave Desert segment of the Cordilleran arc (e.g., Dickinson et al., 2012).

Figure 8 (*on following two pages*). Generalized paleogeographic reconstruction of the Cenomanian–Eocene continental margin. The ages of potential source rocks are generalized from Figure 2. Detrital zircon U-Pb age populations are shown as pie diagrams (see Fig. 7 for key). Hypothetical fluvial-submarine sediment dispersal pathways are shown as blue lines. The continental drainage divide is shown as a dashed black line. The approximate location of an inferred oceanic plateau is from Liu et al. (2010). The relative plate motion between the Farallon and Pacific plates is shown as a black arrow with convergence velocity indicated (Cenomanian–Coniacian—Liu et al., 2008; Santonian–Eocene—Doubrovine and Tarduno, 2008). Aspects of this reconstruction are modified from the following data sources: Dickinson et al. (1979); Ingersoll (1979); Nilsen and Abbott (1981); Kies and Abbott (1982); Sundberg and Cooper (1982); DeGraaff-Surpless et al. (2002); Dickinson et al. (2012); Sharman et al. (2013); Surpless and Beverly (2013). See Figure 2 for abbreviated forearc sample locations. Abbreviations: NCB—Nacimiento block; DR—Dome Rock; MM—McCoy Mountains retroarc; RF—retroarc foreland; SB—Salinian block; WTR—Western Transverse Ranges.

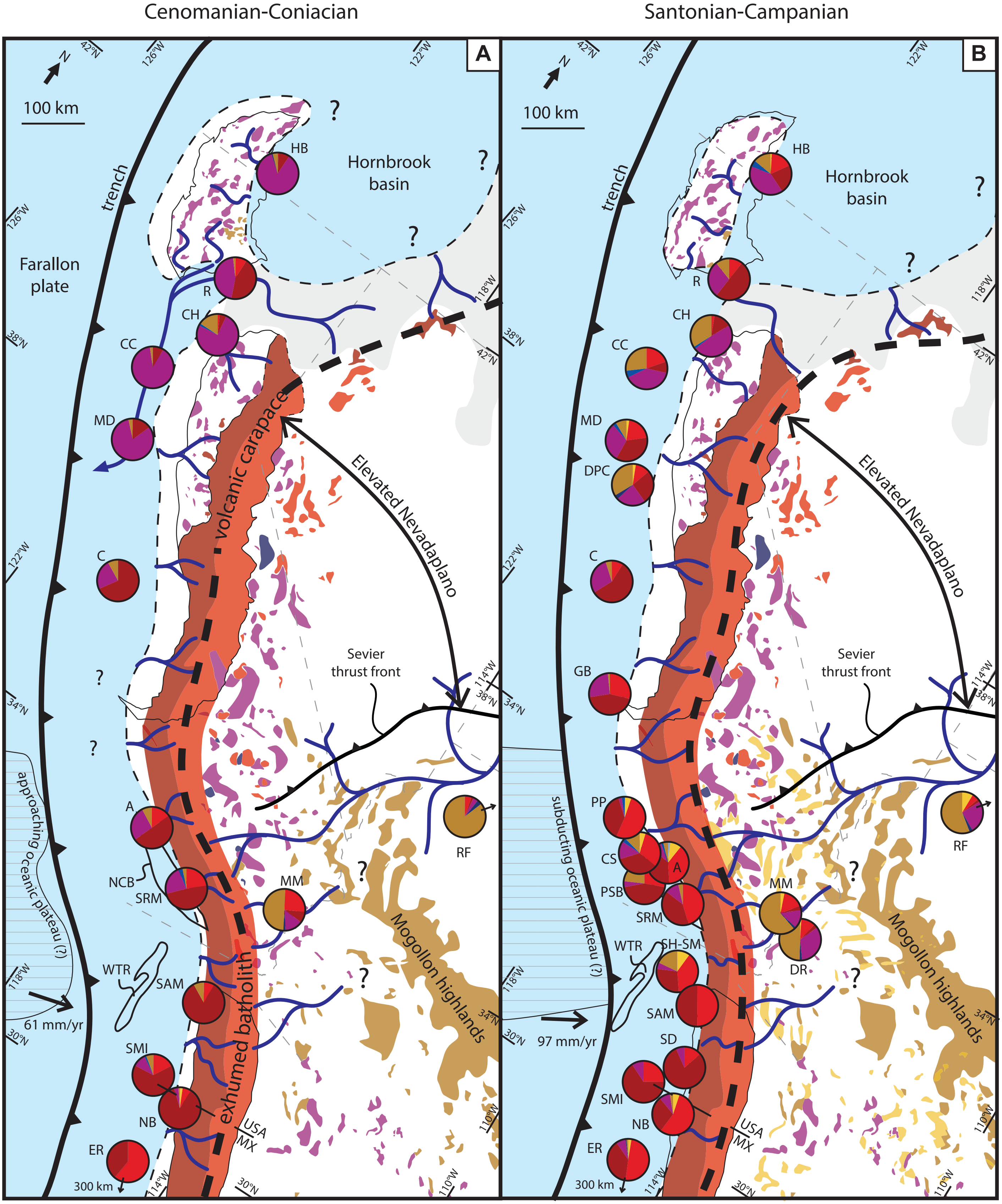
Cenomanian-Coniacian
Santonian-Campanian
A
B
N
100 km
trench
Farallon plate
Hornbrook basin
?
HB
R
CH
CC
MD
DPC
C
GB
volcanic carapace
Elevated Nevadaplano
Sevier thrust front
RF
A
PP
CS
PSB
NCB
SRM
MM
DR
WTR
SAM
SH-SM
SD
SMI
NB
ER
300 km
exhumed batholith
Mogollon highlands
approaching oceanic plateau (?)
subducting oceanic plateau (?)
61 mm/yr
97 mm/yr
USA
MX
42°N
38°N
34°N
30°N
126°W
122°W
118°W
114°W
110°W

Figure 8.

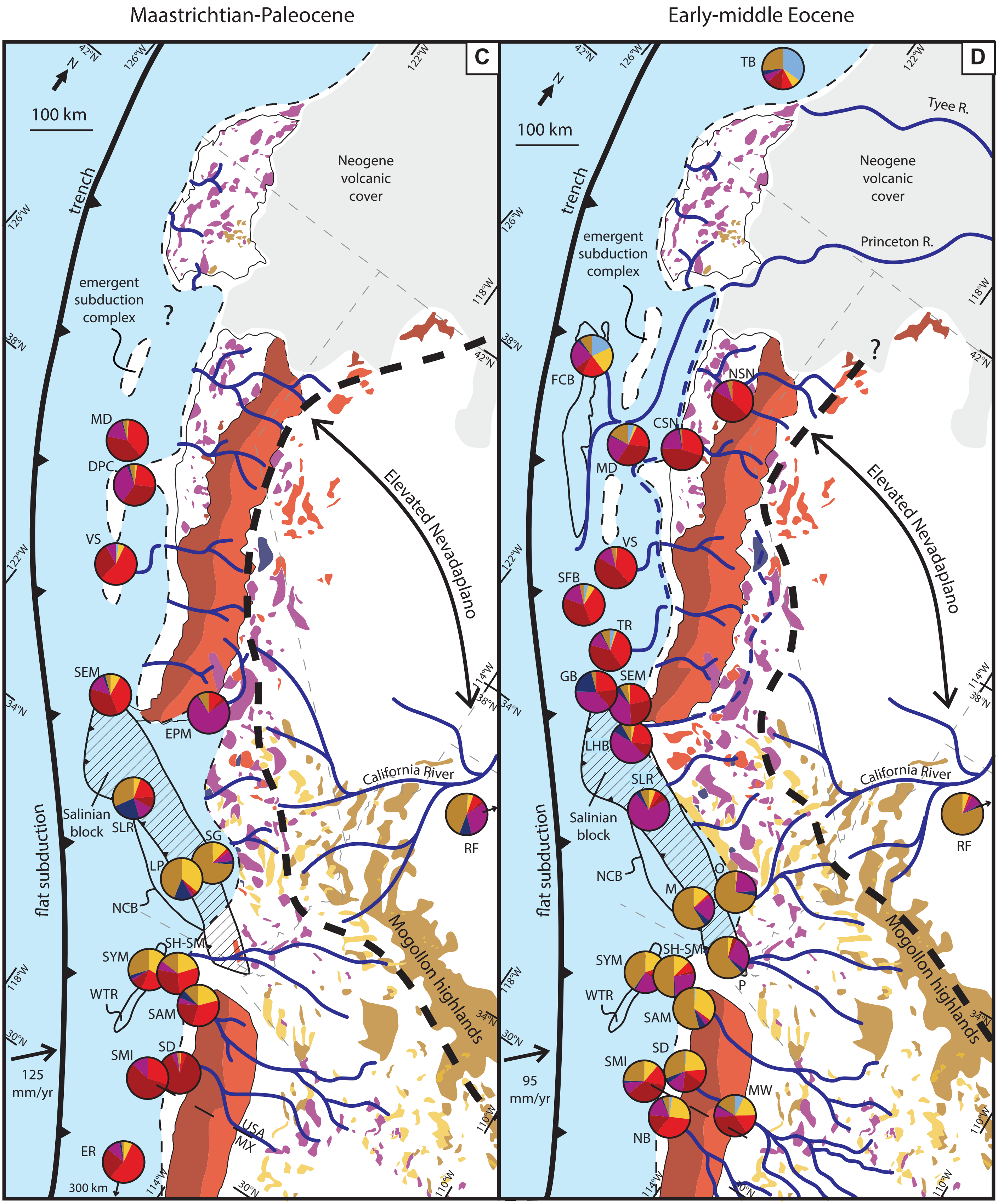

Figure 8 (*continued*).

This interpretation is supported by comparison of the detrital zircon age distributions from the Colton Formation with time-equivalent forearc strata from the Salinian block, Transverse Ranges, and Peninsular Ranges (Fig. 6). Latest Cretaceous zircon (ca. 85–65 Ma) is present in both the Colton Formation and in the Transverse Ranges forearc, although Triassic–Jurassic zircon is an important age population present in the Colton Formation that is nearly absent in Maastrichtian–Paleocene forearc strata (Fig. 6). Extension of the California River headwaters into the western Mojave Desert region is supported by comparison with the Paleocene intra-arc Goler basin and Eocene Salinian forearc, which contain abundant Jurassic zircon (Figs. 6, 8C, and 8D). Triassic zircon is also present in modest abundances in strata from the Salinian block and most notably comprises up to 22% of the early Eocene German Rancho Formation (Gualala block) and up to 50% of Maastrichtian–Paleocene strata in the Santa Lucia Range (Figs. 3D and 7; Barbeau et al., 2005; Doebbert et al., 2012). Thus, the hypothetical California River drainage is inferred to have extended headward as far as the western Mojave Desert region, where Triassic–Jurassic igneous rocks are known to have been a local source to the forearc (Figs. 8C and 8D).

Lower to Middle Eocene Forearc (56–36 Ma)

Lower to middle Eocene forearc strata display systematic north-south trends in sedimentary provenance that reflect the culmination of inboard sediment delivery to the continental margin and the age distribution of igneous rocks along both the intact and breached segments of the mid-Cretaceous Cordilleran arc (Figs. 7 and 8D). In general, distinct assemblages of detrital zircon age populations were derived from at least five adjacent fluvial systems with headwaters that extended into (1) north-central Idaho (Tyee and Princeton Rivers; Dumitru et al., 2012), (2) the Sierra Nevada batholith (Cecil et al., 2010; Cassel et al., 2012), (3) the western Mojave region (Lechler and Niemi, 2011), (4) the eastern Mojave Desert and Mogollon highlands (Jacobson et al., 2011), and (5) Sonoran Desert and southwestern Arizona (Jacobson et al., 2011).

1. Idaho batholith and adjacent volcanic fields. Eocene extensional deformation and associated uplift and erosion in north-central Idaho (ca. 53–40 Ma; Foster et al., 2007) produced abundant sediment derived from the Idaho batholith and Challis volcanic field that reached the Oregon and California forearc via the Tyee and Princeton Rivers (Fig. 8D; Dumitru et al., 2012). The Paleocene–early Eocene Princeton submarine canyon for a time conveyed Idahoan detritus down the axis of the Sacramento basin to the Mount Diablo area, which has formed a persistent depocenter in the Great Valley forearc since Cretaceous time (Moxon, 1990). From this point, Idahoan detritus was longitudinally dispersed to the north and south in trench-slope basins (e.g., Underwood, 1983; Snow et al., 2010) and eventually to the trench, where a mixture of Sierran- and Idahoan-derived sediment was subducted and accreted during early Eocene time to form the Franciscan Coastal belt (Dumitru et al., 2012). Paleogene zircon is found as far south as the Temblor Range (Sharman et al., 2013), suggesting that the Idahoan sediment dispersal system was active over the entire length of the Eocene Great Valley forearc.

2. Sierra Nevada. Aside from variable contribution from sediment sources in Idaho, Eocene sandstone in the Great Valley forearc is characterized by a laterally consistent provenance signature for over ~400 km that is indistinguishable from age distributions in Maastrichtian–Paleocene Great Valley strata (Figs. 3C, 3D, 5, and 7). These sandstone samples are dominated by mid-Cretaceous (ca. 125–85 Ma) zircon with a characteristically asymmetrical distribution (peak at ca. 97 Ma; Fig. 3D), have lesser abundances of Jurassic–earliest Cretaceous zircon (Fig. 7), and are interpreted to have been derived from both the western and eastern portions of the Sierra Nevada batholith (Fig. 8D). This signature is present in westward-draining fluvial systems that are preserved in the northern Sierra Nevada and indicate significant topography of the ancestral Sierra Nevada Mountains (Mulch et al., 2006; Cecil et al., 2010; Cassel et al., 2012). Similar west-flowing drainages are likewise inferred in the southern Sierra Nevada (Fig. 8D), although incised channels have not been identified and are likely no longer preserved (Henry et al., 2012). Sierran detritus was distributed to the adjacent shelfal and deep-water forearc via incised valleys and submarine canyons cut into the Sierran shelf edge (Graham and Berry, 1979; Sullivan and Sullivan, 2012). Uplift and emergence of the Franciscan subduction complex along the western margin of the San Joaquin basin (Schulein, 1993) helped partition thick successions of sand-rich turbidite deposits into structurally controlled, ponded depocenters (e.g., Cantua Sandstone and Point of Rocks Sandstone; Nilsen et al., 1974; Nilsen and Clarke, 1975; Graham and Berry, 1979). Sierran detritus was subsequently delivered from the forearc to trench-slope basins preserved atop the San Francisco Bay block through an outlet that is inferred to have existed in the trench-slope break (Fig. 8D).

3. Western Mojave region. A major provenance shift occurred in the southernmost San Joaquin basin at ~35° latitude, where an influx of Late Permian–Jurassic zircon to the margin indicates that forearc drainages extended eastward to the western Mojave Desert and/or southeastern Sierra Nevada regions (Figs. 7 and 8D; Lechler and Niemi, 2011; Doebbert et al., 2012; Sharman et al., 2013). Forearc strata deposited atop the northern and central Salinian block are dominated by Jurassic zircon (36%–73%), with lesser proportions of Permian–Triassic zircon (4%–20%), which indicate derivation from older arc segments that occurred inboard of the mid-Cretaceous arc (Figs. 2 and 7). In particular, the importance of a Jurassic-aged source region along this portion of the margin is evident in the northern Santa Lucia Range, where Jurassic zircon comprises a large proportion (70%–92%) of the middle Eocene The Rocks Sandstone (Figs. 3D and 7). Maastrichtian–Paleocene forearc strata in these same areas lack abundant Jurassic zircon, suggesting that this sediment dispersal system did not supply detritus to the forearc until early Eocene time (Figs. 8C and 8D). The cause of the influx of Jurassic grains to the forearc is enigmatic but may have resulted from either increased uplift and denudation in the hinterland or an eastward migration of forearc drainages into the western Mojave Desert region during Eocene time (Fig. 8D).

An important aspect of our paleogeographic reconstruction is the inference that strata deposited atop the northern and central Salinian block were derived, in large part, from drainages that extended inboard of the mid-Cretaceous arc (Fig. 8). This interpretation departs from previous models (e.g., Nilsen and Clarke, 1975), which have inferred the central California margin to be characterized by “continental borderland” topography with local, uplifted crustal blocks providing sediment to adjacent, bathyal basins (see also discussion in Grove, 1993; Jacobson et al., 2011). Derivation from local exposures of the Salinian block would yield detrital zircon age distributions dominated by mid- to Late Cretaceous zircon (ca. 110–76 Ma; Mattinson, 1990; Figs. 4 and 5). However, detrital zircon age distributions of Cretaceous–Eocene Salinian forearc sandstone are markedly dissimilar to the distribution of zircon U-Pb ages from Salinian basement (Fig. 5). Instead, the abundance of pre–135 Ma zircon in Eocene successions deposited atop the Salinian block suggests that these strata were sourced in large part from regions to the east (Fig. 8D). In addition, widespread marine sedimentation atop the Salinian block during Paleogene time (Nilsen and Clarke, 1975; Graham, 1976a, 1976b) suggests that this terrane was largely submerged during this time period (Fig. 8D). For these reasons, the Salinian block was likely not a major sediment source to adjacent Paleogene forearc depocenters.

4. Eastern Mojave region and Mogollon highlands. Another abrupt provenance shift occurred south of the central Salinian block, where mid-Cretaceous zircon becomes nearly absent and is replaced by Proterozoic and Jurassic zircon populations that are found in the Transverse Ranges forearc (Sierra Madre Mountains, Pine Mountain block, and Orocopia Mountains; Figs. 7 and 8D; Jacobson et al., 2011). Similar distributions are found in forearc strata from the Santa Ynez Mountains, Simi Hills, and Santa Monica Mountains, although these regions also include populations of latest Cretaceous (ca. 85–65 Ma) zircon. These strata were likely sourced from the eastern Mojave Desert and Mogollon highlands region of southwestern Arizona, based on the occurrence of Jurassic and latest Cretaceous plutons that intrude Proterozoic crustal rocks with age peaks at ca. 1.4 and 1.7 Ga in these regions (Jacobson et al., 2011).

5. Sonoran Desert and southwestern Arizona. Detrital zircon age distributions in the Peninsular Ranges forearc are consistent with studies of conglomerate clast compositions that indicate that drainages extended across the northern Peninsular Ranges batholith into the Sonoran Desert region and southwestern Arizona (Abbott and Smith, 1978, 1989). Additional populations of mid-Cretaceous zircon from forearc strata in the San Diego area and northern Baja California indicate local contribution from the Peninsular Ranges batholith (Figs. 7 and 8D). Detrital zircon age distributions from the late Eocene Ballenas Gravels are similar to those in the San Diego area, supporting the interpretation of a through-going fluvial network (Fig. 8D). In general, the amount of extra-regional detritus decreases southward along the Peninsular Ranges forearc, suggesting increasing isolation from inboard source regions in this direction (Figs. 7 and 8D).

Forearc–Subduction Complex–Underplated Schist Comparison

Detritus delivered to the continental margin that was able to bypass the forearc and eventually reach the trench was either accreted to the margin as part of the Franciscan subduction complex (Dumitru et al., 2010) or underplated beneath the margin to form metasedimentary schist (e.g., Pelona-Orocopia-Rand schist; Grove et al., 2003a). In some cases, detrital zircon age distributions in the forearc closely match those in the adjacent subduction complex or underplated schist (e.g., compare Transverse and Peninsular Ranges forearc with age-equivalent underplated schist; Fig. 6; see also discussion in Jacobson et al., 2011). However, we also observe that adjacent forearc and subduction complex segments can display markedly different detrital zircon age distributions. For example, the Eocene Franciscan subduction complex has a very different age distribution than that found in the adjacent Sacramento basin (Figs. 2 and 6). Samples from the Franciscan subduction complex inferred to be Cenomanian–Coniacian in age display the prominent Late Jurassic peak present in the Sacramento basin but also contain Early Cretaceous ages found in the San Joaquin basin (Fig. 6). Similarly, three Santonian–Campanian(?) Franciscan samples from Pacheco Pass (Ernst et al., 2009) and Marin County (Prohoroff et al., 2012) broadly resemble those from the Great Valley forearc but are enriched in post–100 Ma zircon relative to time-equivalent forearc strata (Fig. 6).

These observed mismatches in forearc–subduction complex provenance can be interpreted as manifestations of longitudinal transport of sand along trench-slope basins and trench floors from variably spaced entry points. This pattern of sediment dispersal is ubiquitous in modern trenches (Underwood and Moore, 1995) and can introduce a detrital zircon age mismatch between forearc basins and their associated subduction complexes. This pattern is well exhibited in the Eocene Franciscan Coastal belt, which has a distinct provenance character from the adjacent forearc because of the delivery of abundant Idahoan detritus that reached the trench via an entry point in the vicinity of Mount Diablo (Dumitru et al., 2012). Alternatively, these differences could be explained by margin-parallel dextral transport of the Franciscan subduction complex relative to the adjacent forearc (Ernst et al., 2009).

Influence of Underlying Geometry of the Jurassic and Mid-Cretaceous Arcs on the Evolution of Forearc Detrital Zircon Age Distributions

One of the most striking aspects of the evolution of detrital zircon age distributions over time in the California forearc is the abundance of Jurassic–earliest Cretaceous (200–135 Ma) zircon in the Great Valley forearc during Cenomanian–Coniacian time, the subsequent decline of this age population relative to mid-Cretaceous zircon, and the following resurgence of Jurassic zircon in the Salinian block and Transverse Ranges in Eocene time (Figs. 3 and 7). This first-order pattern is a clear reflection of the underlying geometry of the Jurassic–earliest Cretaceous and mid-Cretaceous arcs; specifically, the latter crosscuts the former, thereby partitioning preserved Jurassic–earliest Cretaceous source rocks into regions inboard and outboard of the younger mid-Cretaceous arc (Figs. 1 and 2). The systematic southward decrease of 200–135 Ma zircon in the Coniacian–Campanian forearc (Fig. 7) is a consequence of Jurassic-aged arc rocks primarily lying outboard of the mid-Cretaceous arc in the north (Klamath Mountains and Sierra Nevada Foothills belt) and inboard of the mid-Cretaceous arc in the south (southeastern Sierra Nevada, Mojave Desert, and Sonoran Desert regions; Figs. 1 and 2). For this reason, Jurassic zircon is uncommon in the southern California forearc (<35°N latitude; Fig. 7) until Eocene time, when forearc drainages were able to locally extend far enough inland to tap the inboard Jurassic arc (Fig. 8D).

Why Is Post–100 Ma Zircon Scarce in the Cenomanian–Coniacian Great Valley Forearc?

An important characteristic of the Cenomanian–Coniacian forearc is the scarcity of contemporaneous zircon, particular in the Hornbrook and Great Valley forearc segments (0%–15%, median 2%), despite being deposited synchronously with a major flare-up (ca. 100–85 Ma) in the adjacent mid-Cretaceous arc (Figs. 3A and 7; Ducea, 2001). The post–100 Ma Sierra Crest intrusive suite accounts for more than 50% of the present exposures of the Sierra Nevada batholith (Fig. 2; Coleman and Glazner, 1997; Ducea, 2001), and zircon of this age is abundant (up to 44%) in modern rivers that drain the Sierra Nevada (Kimbrough et al., 2009). The near absence of age-equivalent zircon in the forearc is quite surprising, particularly because both petrographic and geochemical studies have suggested that the Sierra Nevada arc was a major source to the contemporaneous Great Valley forearc (Ingersoll, 1983; Linn et al., 1992).We see three potential explanations:

(1) A drainage divide may have existed west of the active volcanic arc that prevented detritus from the volcanic carapace from being delivered to the adjacent forearc basin (DeGraaff-Surpless et al., 2002, their Fig. 12B). The presence of a drainage divide wholly west of the mid-Cretaceous arc is precluded by petrographic and geochemical evidence, which indicates that forearc sandstone contains andesitic detritus derived from the volcanic carapace of the mid-Cretaceous arc (Ingersoll, 1983; Linn et al., 1992). However, the lack of post–100 Ma detrital zircon could suggest that the western, pre–100 Ma arc was a major source to the forearc, while the volcanic carapace of the eastern, post–100 Ma volcanic arc was largely partitioned from the forearc (Fig. 2). Modern silicic calderas that form in continental arcs tend to be preferentially located behind the arc front (Hughes and

Mahood, 2011) and thus are more likely to be a source to the retroarc region rather than to the forearc. Some support for this interpretation is provided by the observation that Cenomanian–Coniacian retroarc sandstones are enriched in post–100 Ma zircon relative to their forearc counterparts (Fig. 6). In addition, local absence of mid-Cretaceous zircon in the western Sacramento basin (Fig. 3A) can be explained by predominantly southward-directed, longitudinal sediment transport during this time period (Ingersoll, 1979). In this case, major sediment contribution to the forearc was likely from the Klamath Mountains to the north, with lesser contribution from the mid-Cretaceous arc in the Sierra Nevada (Fig. 8A; DeGraaff-Surpless et al., 2002).

(2) The post–100 Ma volcanic arc may have been a source to the Great Valley forearc but yielded little zircon. This interpretation hinges on the inference that felsic to intermediate volcanic rocks yield fewer and smaller zircon grains than their plutonic counterparts (Poldervaart, 1956; Watson, 1979). However, this inference is at odds with the abundance of Early Cretaceous zircon in Upper Cretaceous samples with high volcanic lithic contents that are inferred to have been derived from the volcanic carapace of the mid-Cretaceous arc (e.g., Grabast and Los Gatos petrofacies; Ingersoll, 1983; DeGraaff-Surpless et al., 2002).

(3) The paucity of post–100 Ma zircon in the Cenomanian–Coniacian forearc may reflect an absence of volcanic equivalents to the ca. 98–86 Ma Sierra Crest intrusive suite. However, although relatively few mid-Cretaceous volcanic sequences have been identified in the Sierra Nevada, the Minarets and Merced Peak caldera complexes provide well-preserved examples of ca. 100 to ≥93 Ma volcanism likely associated with the voluminous Sierra Crest intrusive event (Fiske and Tobisch, 1994; Lowe, 1996). In addition, the presence of volcanic ash deposits of this age in retroarc foreland sequences (e.g., Cadrin et al., 1996) confirms the existence of extrusive, silicic volcanism during Late Cretaceous time.

Regardless of the specific reason why post–100 Ma zircon is so scarce in the Cenomanian–Coniacian forearc, we interpret the gradual influx of this age population during Santonian to Paleogene time to signal the progressive erosion into plutons of the Sierra Crest intrusive suite (Figs. 3B–3D, 5, and 7).

Influence of Low-Angle Subduction on the Evolution of an Arc-Forearc System

The Laramide orogeny is widely considered to have resulted from low-angle subduction that accompanied the collision and subsequent subduction of an oceanic ridge or plateau beneath North America (Livaccari et al., 1981; Henderson et al., 1984; Saleeby, 2003). Potential candidates include the conjugates to the Hess and Shatsky Plateaus of the present-day northwest Pacific (Tarduno et al., 1985). Both plate motion reconstructions and inverse convection models predict that the Shatsky conjugate plateau collided with the North American plate at ca. 90 Ma in the vicinity of southern California (Liu et al., 2010). We hypothesize that major spatial and temporal trends in forearc sandstone provenance were greatly influenced by the impingement of the Shatsky conjugate plateau on the continental margin, and that this event resulted in both differential uplift and denudation of the mid-Cretaceous volcanic-plutonic arc and eventual breaching of an ~500 km segment of the southern California mid-Cretaceous margin batholith (e.g., Saleeby, 2003).

Contrasting Denudation History of the Sierran and Peninsular Ranges Batholiths

Although the Sierran and Peninsular Ranges segments of the mid-Cretaceous batholith share many commonalities in their magmatic history (e.g., Chen and Moore, 1982; Silver and Chappell, 1988), they differ significantly in the magnitude, distribution, and timing of postmagmatic uplift and denudation (Ague and Brimhall, 1988; George and Dokka, 1994; Grove et al., 2003b; Saleeby et al., 2007, 2008). Major differences in detrital zircon age distributions between the Great Valley and Peninsular Ranges segments of the forearc (Fig. 5) can be understood to be a consequence of these contrasting denudation histories, in addition to the underlying control contributed by the crosscutting geometry of the mid-Cretaceous arc relative to older arc segments.

The Peninsular Ranges underwent rapid denudation following emplacement of the 99–92 Ma La Posta suite that caused an influx of coarse detritus to the Cenomanian–Turonian forearc and resulted in detrital zircon age distributions that exhibit little time lag between U-Pb crystallization and depositional ages (Kimbrough et al., 2001; Grove et al., 2003b; Fig. 3A). The timing of denudation (ca. 91–86 Ma) corresponds closely with the predicted time (ca. 90 Ma) and location of plateau collision with the margin (Grove et al., 2003b; Liu et al., 2010), suggesting that these two events were causally linked. Alternatively, mechanical and thermal effects related to high rates of magmatic flux during the La Posta intrusive event could have also contributed to denudation of the Peninsular Ranges arc (Kimbrough et al., 2001; Grove et al., 2003b). Regardless of the mechanism, depths of the modern level of erosion in the northern Peninsular Ranges batholith (0–8 km in the west and typically 12–20 km in the east; Ague and Brimhall, 1988; Herzig and Kimbrough, 2014) were nearly attained by latest Cretaceous time (George and Dokka, 1994; Grove et al., 2003b, 2008). As a result, detrital zircon age distributions of Cenomanian–Paleocene forearc strata essentially match the distribution of U-Pb ages from the modern surface of the Peninsular Ranges batholith and exhibit little change over time until the delivery of inboard detritus to the margin in Eocene time (Figs. 5, 8C, and 8D).

The Great Valley forearc exhibits a very different provenance evolution, where Cenomanian–Paleocene forearc strata exhibit increasing abundances of 125–85 Ma zircon over time that are interpreted to reflect progressive denudation of the Sierra Nevada batholith (Fig. 5). Cenomanian–Coniacian strata display comparatively larger time lags between peak detrital zircon U-Pb ages and depositional ages, despite voluminous concurrent magmatism to the east (Fig. 3A). The influx of 100–85 Ma zircon to the forearc at the Coniacian-Santonian boundary (Fig. 3B) likely relates to the attainment of erosional depths great enough to expose plutons of the Sierra Crest intrusive suite in the eastern Sierra Nevada batholith and coincides with a cooling event in the western Sierra Nevada (Cecil et al., 2006; Saleeby et al., 2010; Surpless and Beverly, 2013). This inference is supported by sandstone petrography and geochemistry, which also signal unroofing of Sierra Nevada batholith during this time interval (Ingersoll, 1983; Linn et al., 1992). Surprisingly, this pulse of denudation coincides with a decrease in sedimentation rates in the Sacramento basin (Williams, 1997), although evidence for sediment transport via incised submarine canyons suggests that any pulse of sedimentation may have bypassed the preserved portion of the Great Valley forearc (Williams et al., 1998; Williams and Graham, 2013).

Although the ca. 98–86 Ma Sierra Crest intrusions account for a majority of present-day exposure of the Sierra Nevada batholith (Coleman and Glazner, 1997; Ducea, 2001), detrital zircon grains of this age do not become abundant in the forearc until Maastrichtian–Paleocene time, suggesting a time lag of at least ~13 m.y. between final pluton emplacement and sufficient arc denudation and erosion to expose the full width of the batholith (Figs. 3C and 5). Modern levels of erosion in the eastern and northern Sierra Nevada batholith (<4 km; Ague and Brimhall, 1988) include volcanic levels of arc crust (e.g., Minarets caldera; Fiske and Tobisch, 1994), are significantly less than those in the eastern Peninsular Ranges batholith (typically 12–20 km; Ague and Brimhall, 1988), and were attained over a much longer period of time. As a result, the eastern batholithic signature that is present in the ca. 90 Ma Peninsular Ranges forearc is not found in the Great Valley forearc until ca. 70 Ma (Fig. 5).

We hypothesize that the contrasting denudation history of the Sierra Nevada and Peninsular Ranges relates to the location of plateau collision with the margin. Specifically, regions proximal to the collision site (i.e., southernmost Sierra Nevada and northern Peninsular Ranges) experienced higher magnitudes and rates of ca. 90 Ma denudation than regions farther away from the collision site (i.e., central and northern Sierra Nevada; Grove et al., 2003b; Saleeby et al., 2007, 2010). This interpretation helps to explain why the Great Valley and Peninsular Ranges forearc segments display opposite trends in detrital zircon age distributions over time despite developing in comparable tectonic settings (Fig. 5). Great Valley forearc age distributions progressively become more similar to the age distribution of plutons in the Sierra Nevada batholith as a result of progressive arc uplift and denudation during Late Cretaceous–early Paleogene time (Fig. 5; Cecil et al., 2006). This contrasts with age distributions in the Peninsular Ranges forearc, which initially were very similar to the age distribution of plutons in the Peninsular Ranges batholith but become less so during Eocene time as fluvial systems bypassed the local batholith and delivered extraregional detritus to the margin (Figs. 5 and 8). Because rapid denudation favors small time lags between U-Pb crystallization and depositional ages, the youngest zircons can provide a close approximation of depositional age for strata sourced from a rapidly unroofing arc (e.g., Kimbrough et al., 2001) but can be considerably older for unroofed or shallowly denuded volcanic arcs (e.g., Cenomanian–Coniacian strata in Cache Creek; DeGraaff-Surpless et al., 2002).

Geomorphic Breaching of the Southern California Margin Batholith

The pronounced and sudden influx of inboard detritus to the southern California margin at ca. 75 Ma (Fig. 7) is a clear reflection of the development of a geomorphic breach within the mid-Cretaceous arc and an associated rapid migration of forearc drainages into the continental interior (Fig. 8). Although these events have been linked with the collision of an oceanic plateau or aseismic ridge with the southern California margin (e.g., Saleeby, 2003; Jacobson et al., 2011), the outboard-to-inboard provenance transition observed in the forearc likely postdated the initial oceanic plateau collision by ~15 m.y. (Fig. 8). By ca. 75 Ma, the Shatsky conjugate plateau is predicted to have been positioned beneath the Colorado Plateau region (Liu et al., 2010). This suggests that the geomorphic breaching of the mid-Cretaceous arc and associated inland drainage migration (Fig. 8) were more likely related to the passage of the oceanic plateau beneath the continental interior than to its initial collision with the margin.

Forearc detrital zircon age distributions clearly demarcate the north-south extent of inboard detritus along the margin and demonstrate that the outboard-to-inboard provenance transition migrated both to the north and south through Maastrichtian–Eocene time (Fig. 7). This pattern is consistent with a localized collision of the oceanic plateau along an ~500 km length of the southern California margin (Figs. 7 and 8; Saleeby, 2003). North-to-south variability within the extraregional provenance signature is related to the distribution of source regions inboard of the mid-Cretaceous arc, rather than from the mid-Cretaceous arc itself (Figs. 7 and 8).

In contrast, provenance trends in areas to the north and south of the oceanic plateau collision (Sierra Nevada and Peninsular Ranges segments) still reflect derivation from the adjacent batholith until drainages migrated to the east to allow extraregional detritus to reach the forearc (Figs. 7 and 8; Cassel et al., 2012). Contrasting denudation histories between the Sierra Nevada and Peninsular Ranges batholiths may have influenced the timing of inboard drainage migration, which occurred earlier (late Paleocene–early Eocene; Kies and Abbott, 1982) in the Peninsular Ranges than in the Sierra Nevada (late Eocene–Oligocene; Cassel et al., 2012). The preservation of the Great Valley and Peninsular Ranges forearc segments can be interpreted to be a consequence of slab segmentation (Saleeby, 2003), which allowed subduction accretion along the Great Valley forearc while the Salinian-Mojave segment of the margin underwent tectonic underplating and subduction erosion (sensu Von Huene and Scholl, 1991). Finally, the influx of Idahoan detritus to the Eocene Tyee and Great Valley forearcs and Franciscan Coastal belt demonstrates that far-field tectonism also contributed to shaping forearc provenance trends (Dumitru et al., 2012).

Influence on Future Development of the San Andreas Fault System

One of the lasting legacies of Laramide flat subduction on the California margin was its influence on preconditioning the later development of the modern Pacific–North American plate boundary. Following tectonic restructuring of the margin batholith in southern California, the Salinian-Mojave segment of the margin likely formed a western "bulge" in the margin (Johnson and Normark, 1974; Figs. 8C and 8D). This vulnerable position would later be exploited by strike-slip faults of the San Andreas system that translated and extended the Salinian block and adjacent crustal pieces of the Mojave Desert region (e.g., the San Gabriel block) northward (Atwater, 1989). Strictly speaking, these processes could have begun immediately following the tectonic restructuring of the margin, inasmuch as dextral obliquity of subduction may have promoted trench-parallel faulting (Fig. 8D; Doubrovine and Tarduno, 2008; Sharman et al., 2013, their Fig. 4). This mechanism may account for the ~100 km of late Paleogene northward translation of the Salinian block that is required by our reconstruction (Sharman et al., 2013; Fig. 2A). Additional northward displacement followed Pacific–North American plate contact (ca. 28–26 Ma) and development of the modern San Andreas system, which resulted in >550 km of cumulative northward translation of portions of the Salinian block (Fig. 2; Atwater, 1989; Dickinson et al., 2005).

CONCLUSIONS

Spatial and temporal trends in sedimentary provenance within in the California forearc can be understood as manifestations of Laramide low-angle subduction and associated oceanic plateau subduction in the landscape evolution of the western U.S. continental margin. As such, our results yield important insights into the tectonic evolution of a well-studied arc-forearc system.

In general, pre-Maastrichtian detrital zircon age distributions demonstrate the existence of a drainage divide formed by a high-standing mid-Cretaceous Cordilleran arc that effectively shielded the forearc from inboard sediment source regions. North-south trends in detrital zircon age distributions can be explained in terms of the primary, crosscutting geometry between the mid-Cretaceous and older arc segments and along-strike, differential uplift and denudation of the mid-Cretaceous batholith that are hypothesized to be related to the initial impingement of an oceanic plateau on the continental margin.

A pronounced transition from local to extraregional provenance in the Maastrichtian–Eocene southern California forearc indicates that a geomorphic breach developed within the formerly high-standing mid-Cretaceous arc that allowed forearc drainages to migrate into the continental interior. These events likely postdated the initial collision of the Shatsky conjugate plateau with the margin by ~15 m.y., suggesting that breaching of the southern California margin was more likely related to the passage of the subducted oceanic plateau beneath the continental interior than to its initial collision with the margin. Forearc strata north and south of the breached margin continued to be derived from the adjacent mid-Cretaceous batholith until progressive eastward drainage migration allowed extra-regional detritus to be delivered to the forearc.

The California forearc provides a case study of the utility of detrital zircon geochronology in resolving landscape evolution in an active margin setting. When applied to arc-adjacent depocenters, detrital zircon provenance analysis allows high-resolution discrimination of potential source regions in a way that is not possible using traditional petrographic techniques alone. This is particularly true where the source regions are segments of a volcano-plutonic arc complex with distinct and well-documented spatial variations in crystallization age. We found the relative abundances of arc-derived age populations to be a sensitive indicator of provenance, in addition to the presence or absence of distinctive age populations. Thus, detrital zircon geochronology constitutes a valuable tool for understanding the tectonic and paleogeographic evolution of arc-forearc systems.

ACKNOWLEDGMENTS

Funding for detrital zircon analyses was provided by the Stanford Project on Deep-Water Depositional Systems, the Stanford School of Earth Sciences Chevron Fund, the Department of Geological Sciences at San Diego State, and the National Science Foundation grant EAR-0409869. Facilities at the Arizona Laserchron Center and the University of California are funded by the National Science Foundation's Instrumentation and Facilities Division and Major Research Instrumentation programs, respectively. We thank the Wildlands Conservancy and B. Cotton for granting access to private land, R. McLaughlin and R. Stanley for assistance with sample collecting in the Sierra Azul block of the Santa Cruz Mountains, K. Baldwin for assistance with collecting the "Quad Sandstone" at Stanford University, and P. Abbott for assistance with collection of Upper Cretaceous and Paleocene Peninsular Ranges and Channel Island samples. This study benefited from discussion with P. Abbott, I. Alarik, A. Almgren, A. Barth, E. Brabb, E. Cassel, W. Dickinson, A. Doebbert, T. Dumitru, C. Jacobson, M. Johns, G. Mahood, M. Malkowski, R. McLaughlin, E. Miller, J. Saleeby, C. Sine, R. Stanley, J. Wooden, and N. Van Buer. We thank the many individuals that provided assistance with processing, analyzing, and reducing data: B. Burgreen, A. Bernhardt, E. Cassel, W. Chang, M. Coble, T. Dumitru, J. Fosdick, N. Giesler, E. Gottlieb, J. Hourigan, J. Kimbrough, B. Mahoney, K. Maier, M. Malkowski, S. Maatta, T. O'Brien, M. Pecha, N. Sarto, and T. Schwartz. We thank our reviewers, C. Jacobson, K. Surpless, and W. Dickinson, for providing constructive feedback that greatly improved the readability and content of this manuscript.

REFERENCES CITED

Abbott, P.L., and Smith, T.E., 1978, Trace element comparison of clasts in Eocene conglomerates, southwestern California and northwestern Mexico: The Journal of Geology, v. 86, p. 753–762, doi:10.1086/649742.

Abbott, P.L., and Smith, T.E., 1989, Sonora, Mexico, source for the Eocene Poway Conglomerate of southern California: Geology, v. 17, p. 329–332, doi:10.1130/0091-7613(1989)017<0329:SMSFTE>2.3.CO;2.

Ague, J.J., and Brimhall, G.H., 1988, Magmatic arc asymmetry and distribution of anomalous plutonic belts in the batholiths of California: Effects of assimilation, crustal thickness, and depth of crystallization: Geological Society of America Bulletin, v. 100, p. 912–927, doi:10.1130/0016-7606(1988)100<0912:MAAADO>2.3.CO;2.

Atwater, T.M., 1989, Plate tectonic history of the northeast Pacific and western North America, *in* Winterer, E.L., Hussong, D.M., and Decker, R.W., eds., The Eastern Pacific Ocean and Hawaii: Boulder, Colorado, Geological Society of America, Geology of North America, v. N, p. 21–72.

Barbeau, D.L., Jr., Ducea, M.N., Gehrels, G.E., Kidder, S., Wetmore, P.H., and Saleeby, J.B., 2005, U-Pb detrital-zircon geochronology of northern Salinian basement and cover rocks: Geological Society of America Bulletin, v. 117, p. 466–481, doi:10.1130/B25496.1.

Barth, A.P., and Wooden, J.L., 2006, Timing of magmatism following initial convergence at a passive margin, southwestern U.S. Cordillera, and ages of lower crustal magma sources: The Journal of Geology, v. 114, p. 231–245, doi:10.1086/499573.

Barth, A.P., Wooden, J.L., Tosdal, R.M., and Morrison, J., 1995, Crustal contamination in the petrogenesis of a calc-alkalic rock series: Josephine Mountain intrusion, California: Geological Society of America Bulletin, v. 107, p. 201–211, doi:10.1130/0016-7606(1995)107<0201:CCITPO>2.3.CO;2.

Barth, A.P., Wooden, J.L., Grove, M., Jacobson, C.E., and Pedrick, J.N., 2003, U-Pb zircon geochronology of rocks in the Salinas Valley region of California: A reevaluation of the crustal structure and origin of the Salinian block: Geology, v. 31, p. 517–520, doi:10.1130/0091-7613(2003)031<0517:UZGORI>2.0.CO;2.

Barth, A.P., Wooden, J.L., Jacobson, C.E., and Probst, K., 2004, U-Pb geochronology and geochemistry of the McCoy Mountains Formation, southeastern California: A Cretaceous retro-arc foreland basin: Geological Society of America Bulletin, v. 116, p. 142–153, doi:10.1130/B25288.1.

Barth, A.P., Wooden, J.L., Jacobson, C.E., and Economos, R.C., 2013, Detrital zircon as a proxy for tracking the magmatic arc system: The California arc example: Geology, v. 41, p. 223–226, doi:10.1130/G33619.1.

Barton, M.D., Girardi, J.D., Kreiner, D.C., Seedorff, E., Zurcher, L., Dilles, J.H., Haxel, G.B., and Johnson, D.A., 2011, Jurassic igneous-related metallogeny of southwestern North America, *in* Steinger, R.L., and Pennell, B., eds., Great Basin Evolution and Metallogeny: Reno, Nevada, Geological Society of Nevada, p. 373–396.

Bottjer, D.J., and Link, M.H., 1984, A synthesis of Late Cretaceous southern California and northern Baja California paleogeography, *in* Crouch, J.K., and Bachman, S.B., eds., Tectonics and Sedimentation Along the California Margin: Los Angeles, Pacific Section, SEPM (Society for Sedimentary Geology), Book 38, p. 171–188.

Cadrin, A.A.J., Kyser, T.K., Caldwell, W.G.E., and Longstaffe, F.J., 1996, Isotopic and chemical compositions of bentonites as paleoenvironmental indicators of the Cretaceous Western Interior Seaway: Palaeogeography, Palaeoclimatology, Palaeoecology, v. 119, p. 301–320, doi:10.1016/0031-0182(95)00015-1.

Cassel, E.J., Grove, M., and Graham, S.A., 2012, Eocene drainage evolution and erosion of the Sierra Nevada batholith across northern California and Nevada: American Journal of Science, v. 312, p. 117–144, doi:10.2475/02.2012.03.

Cecil, M.R., Ducea, M.N., Reiners, P.W., and Chase, C.G., 2006, Cenozoic exhumation of the northern Sierra Nevada, California, from (U-Th)/He thermochronology: Geological Society of America Bulletin, v. 118, p. 1481–1488, doi:10.1130/B25876.1.

Cecil, M.R., Ducea, M.N., Reiners, P., Gehrels, G., Mulch, A., Allen, C., and Campbell, I., 2010, Provenance of Eocene river sediments from the central northern Sierra Nevada and implications for paleotopography: Tectonics, v. 29, TC6010, doi:10.1029/2010TC002717, 13 p.

Centeno-García, E., Guerrero-Suastegui, M., and Talavera-Mendoza, O., 2008, The Guerrero composite terrane of western Mexico: Collision and subsequent rifting in a supra-subduction zone, *in* Draut, A.E., Clift, P.D., and Scholl, D.W., eds., Formation and Applications of the Sedimentary Record in Arc Collision Zones: Geological Society of America Special Paper 436, p. 279–308.

Chapman, A.D., Saleeby, J.B., Wood, D.J., Piasecki, A., Kidder, S., Ducea, M.N., and Farley, K.A., 2012, Late Cretaceous gravitational collapse of the southern Sierra Nevada batholith, California: Geosphere, v. 8, p. 314–341, doi:10.1130/GES00740.1.

Chapman, A.D., Saleeby, J.B., and Eiler, J., 2013, Slab flattening trigger for isotopic disturbance and magmatic flare-up in the southernmost Sierra Nevada batholith, California: Geology, v. 41, p. 1007–1010, doi:10.1130/G34445.1.

Chen, J.H., and Moore, J.G., 1982, Uranium-lead isotopic ages from the Sierra Nevada batholith: Journal of Geophysical Research, v. 87, p. 4761–4784, doi:10.1029/JB087iB06p04761.

Chetel, L.M., Janecke, S.U., Carroll, A.R., Beard, B.L., Johnson, C.M., and Singer, B.S., 2011, Paleogeographic reconstruction of the Eocene Idaho River, North American Cordillera: Geological Society of America Bulletin, v. 123, p. 71–88, doi:10.1130/B30213.1.

Coleman, D.S., and Glazner, A.F., 1997, The Sierra Crest magmatic event: Rapid formation of juvenile crust during the Late Cretaceous in California: International Geology Review, v. 39, p. 768–787, doi:10.1080/00206819709465302.

Coleman, D.S., Bartley, J.M., Glazner, A.F., and Pardue, M.J., 2012, Is chemical zonation in plutonic rocks driven by changes in source magma composition or shallow-crustal differentiation?: Geosphere, v. 8, p. 1568–1587, doi:10.1130/GES00798.1.

Cowan, D.S., and Bruhn, R.L., 1992, Late Jurassic to early Late Cretaceous geology of the U.S. Cordillera, *in* Burchfiel, B.C., Lipman, P.W., and Zoback, M.L., eds., The Cordilleran Orogen: Boulder, Colorado, Geological Society of America, The Geology of North America, v. G-3, p. 169–189.

Cox, B.F., 1982, Stratigraphy, Sedimentology, and Structure of the Goler Formation (Paleocene), El Paso Mountains, California: Implications for Paleogene Tectonism on the Garlock Fault Zone [Ph.D. thesis]: Riverside, California, University of California, 248 p.

Crowell, J.C., 2003, Tectonics of Ridge Basin region, southern California, *in* Crowell, J.C., ed., Evolution of Ridge Basin, Southern California: An Interplay of Sedimentation and Tectonics: Geological Society of America Special Paper 367, p. 157–203.

DeCelles, P.G., 2004, Late Jurassic to Eocene evolution of the Cordilleran thrust belt and foreland basin system, western U.S.A.: American Journal of Science, v. 304, p. 105–168, doi:10.2475/ajs.304.2.105.

DeGraaff-Surpless, K., Graham, S.A., Wooden, J.L., and McWilliams, M.O., 2002, Detrital zircon provenance analysis of the Great Valley Group, California: Evolution of an arc-forearc system: Geological Society of America Bulletin, v. 114, p. 1564–1580, doi:10.1130/0016-7606(2002)114<1564:DZPAOT>2.0.CO;2.

Dickinson, W.R., 1983, Cretaceous sinistral strike slip along Nacimiento fault in coastal California: American Association of Petroleum Geologists Bulletin, v. 67, p. 624–645.

Dickinson, W.R., 1995a, Forearc basins, *in* Busby, C.J., and Ingersoll, R.V., eds., Tectonics of Sedimentary Basins: Cambridge, Massachusetts, Blackwell Science, p. 221–261.

Dickinson, W.R., 1995b, Paleogene depositional systems of the western Transverse Ranges and adjacent southernmost Coast Ranges, California, *in* Fritsche, A.E., ed., Cenozoic Paleogeography of the Western United States—II: Los Angeles, Pacific Section, SEPM (Society for Sedimentary Geology), Book 75, p. 58–83.

Dickinson, W.R., 1996, Kinematics of Transrotational Tectonism in the California Transverse Ranges and its Contribution to Cumulative Slip along the San Andreas Transform Fault System: Geological Society of America Special Paper 305, 46 p.

Dickinson, W.R., 2008, Accretionary Mesozoic-Cenozoic expansion of the Cordilleran continental margin in California and adjacent Oregon: Geosphere, v. 4, p. 329–353, doi:10.1130/GES00105.1.

Dickinson, W.R., and Gehrels, G.E., 2008, Sediment delivery to the Cordilleran foreland basin: Insights from U-Pb ages of detrital zircons in Upper Jurassic and Cretaceous strata of the Colorado Plateau: American Journal of Science, v. 308, p. 1041–1082, doi:10.2475/10.2008.01.

Dickinson, W.R., and Gehrels, G.E., 2009, U-Pb ages of detrital zircons in Jurassic eolian and associated sandstones of the Colorado Plateau: Evidence for transcontinental dispersal and intraregional recycling of sediment: Geological Society of America Bulletin, v. 121, p. 408–433, doi:10.1130/B26406.1.

Dickinson, W.R., and Lawton, T.F., 2001, Carboniferous to Cretaceous assembly and fragmentation of Mexico: Geological Society of America Bulletin, v. 113, p. 1142–1160, doi:10.1130/0016-7606(2001)113<1142:CTCAAF>2.0.CO;2.

Dickinson, W.R., and Seely, D.R., 1979, Structure and stratigraphy of forearc regions: American Association of Petroleum Geologists Bulletin, v. 63, p. 2–31.

Dickinson, W.R., and Snyder, W.S., 1978, Plate tectonics of the Laramide orogeny, *in* Matthews, V., III, ed., Laramide Folding Associated with Basement Block Faulting in the Western United States: Geological Society of America Memoir 151, p. 355–366.

Dickinson, W.R., Ingersoll, R.V., and Graham, S.A., 1979, Paleogene sediment dispersal and paleotectonics in northern California: Geological Society of America Bulletin, v. 90, pt. I, p. 897–898; pt. II, p. 1458–1528.

Dickinson, W.R., Ducea, M., Rosenberg, L.I., Greene, H.G., Graham, S.A., Clark, J.C., Weber, G.E., Kidder, S., Ernst, W.G., and Brabb, E.E., 2005, Net Dextral Slip, Neogene San Gregorio–Hosgri Fault Zone, Coastal California: Geologic Evidence and Tectonic Implications: Geological Society of America Special Paper 391, 43 p.

Dickinson, W.R., Lawton, T.F., Pecha, M., Davis, S.J., Gehrels, G.E., and Young, R.A., 2012, Provenance of the Paleogene Colton Formation (Uinta Basin) and Cretaceous–Paleogene provenance evolution in the Utah foreland: Evidence from U-Pb ages of detrital zircons, paleocurrent trends, and sandstone petrofacies: Geosphere, v. 8, p. 854–880, doi:10.1130/GES00763.1.

Dilles, J.H., and Wright, J.E., 1988, The chronology of early Mesozoic arc magmatism in the Yerington district of western Nevada and its regional implications: Geological Society of America Bulletin, v. 100, p. 644–652, doi:10.1130/0016-7606(1988)100<0644:TCOEMA>2.3.CO;2.

Doebbert, A.C., Carroll, A.R., and Johnson, C., 2012, The sandstone-derived provenance record of the Gualala basin, northern California, U.S.A.: Journal of Sedimentary Research, v. 82, p. 841–858, doi:10.2110/jsr.2012.72.

Dokka, R.K., and Travis, C.J., 1990, Late Cenozoic strike-slip faulting in the Mojave Desert, California: Tectonics, v. 9, p. 311–340, doi:10.1029/TC009i002p00311.

Doubrovine, P.V., and Tarduno, J.A., 2008, A revised kinematic model for the relative motion between Pacific oceanic plates and North America since the Late Cretaceous: Journal of Geophysical Research, v. 113, p. B12101, doi:10.1029/2008JB005585.

Ducea, M., 2001, The California arc: Thick granitic batholiths, eclogitic residues, lithospheric-scale thrusting and magmatic flare-ups: GSA Today, v. 11, no. 11, p. 4–10, doi:10.1130/1052-5173(2001)011<0004:TCATGB>2.0.CO;2.

Ducea, M.N., and Barton, M.D., 2007, Igniting flare-up events in Cordilleran arcs: Geology, v. 35, p. 1047–1050, doi:10.1130/G23898A.1.

Ducea, M.N., Kidder, S., Chesley, J.T., and Saleeby, J.B., 2009, Tectonic underplating of trench sediments beneath magmatic arcs, the central California example: International Geology Review, v. 51, p. 1–26, doi:10.1080/00206810802602767.

Dumitru, T.A., Wakabayashi, J., Wright, J.E., and Wooden, J.L., 2010, Early Cretaceous transition from nonaccretionary behavior to strongly accretionary behavior within the Franciscan subduction complex: Tectonics, v. 29, TC5001, doi:10.1029/2009TC002542.

Dumitru, T.A., Ernst, W.G., Wright, J.E., Wooden, J.L., Wells, R.E., Farmer, L.P., Kent, A.J.R., and Graham, S.A., 2012, Eocene extension in Idaho generated massive sediment floods into the Franciscan trench and into the Tyee, Great Valley, and Green River basins: Geology, v. 41, p. 187–190, doi:10.1130/G33746.1.

Ernst, W.G., Martens, U., and Valencia, V., 2009, U-Pb ages of detrital zircons in Pacheco Pass metagraywackes: Sierran-Klamath source of mid- and Late Cretaceous Franciscan deposition and underplating: Tectonics, v. 28, TC6011, doi:10.1029/2008TC002352.

Fildani, A., Hessler, A.M., and Graham, S.A., 2008, Trench-forearc interactions reflected in the sedimentary fill of Talara basin, northwest Peru: Basin Research, v. 20, p. 305–331, doi:10.1111/j.1365-2117.2007.00346.x.

Fiske, R.S., and Tobisch, O.T., 1994, Middle Cretaceous ash-flow tuff and caldera-collapse deposit in the Minarets caldera, east-central Sierra Nevada, California: Geological Society of America Bulletin, v. 106, p. 582–593, doi:10.1130/0016-7606(1994)106<0582:MCAFTA>2.3.CO;2.

Foster, D.A., Doughty, P.T., Kalakay, T.J., Fanning, C.M., Coyner, S., Grice, W.C., and Vogl, J., 2007, Kinematics and timing of exhumation of metamorphic core complexes along the Lewis and Clark fault zone, northern Rocky Mountains, USA, *in* Till, A.B., Roeske, S.M., Sample, J.C., and Foster, D.A., eds., Exhumation Associated with Continental Strike-Slip Fault Systems: Geological Society of America Special Paper 434, p. 207–232.

Gaschnig, R.M., Vervoort, J.D., Lewis, R.S., and Tikoff, B., 2011, Isotopic evolution of the Idaho batholith and Challis intrusive province, northern U.S. Cordillera: Journal of Petrology, v. 52, p. 2397–2429, doi:10.1093/petrology/egr050.

Gehrels, G.E., Valencia, V.A., and Ruiz, J., 2008, Enhanced precision, accuracy, efficiency, and spatial resolution of U-Th-Pb ages by LA-MC-ICPMS: Geochemistry Geophysics Geosystems, v. 9, Q03017, doi:10.1029/2007GC001805.

George, P.G., and Dokka, R.K., 1994, Major Late Cretaceous cooling events in the eastern Peninsular Ranges, California, and their implications for Cordilleran tectonics: Geological Society of America Bulletin, v. 106, p. 903–914, doi:10.1130/0016-7606(1994)106<0903:MLCCEI>2.3.CO;2.

Graham, S.A., 1976a, Tertiary Sedimentary Tectonics of the Central Salinian Block of California [Ph.D. dissertation]: Stanford, California, Stanford University, 510 p.

Graham, S.A., 1976b, Tertiary stratigraphy and depositional environments near Indians Ranch, Monterey County, California, *in* Fritsche, A.E., Ter Best, H., Jr., and Wornardt, W.W., eds., The Neogene Symposium: Los Angeles, Pacific Section, SEPM (Society for Sedimentary Geology), p. 125–136.

Graham, S.A., 1978, Role of Salinian block in evolution of San Andreas fault system, California: American Association of Petroleum Geologists Bulletin, v. 62, p. 2214–2231.

Graham, S.A., and Berry, K.D., 1979, Early Eocene paleogeography of the central San Joaquin Valley: Origin of the Cantua Sandstone, *in* Armentrout, J.M., Cole, M.R., and Ter Best, H., Jr., eds., Cenozoic Paleogeography of the Western United States: Los Angeles, Pacific Section, SEPM (Society for Sedimentary Geology), Pacific Coast Paleogeography Symposium 3, p. 119–127.

Graham, S.A., Stanley, R.G., Bent, J.V., and Carter, J.B., 1989, Oligocene and Miocene paleogeography of central California and displacement along the San Andreas fault: Geological Society of America Bulletin, v. 101, p. 711–730, doi:10.1130/0016-7606(1989)101<0711:OAMPOC>2.3.CO;2.

Graymer, R.W., Sarna-Wojcicki, A.M., Walker, J.P., McLaughlin, R.J., and Fleck, R.J., 2002, Controls on timing and amount of right-lateral offset on the East Bay fault system, San Francisco Bay region, California: Geological Society of America Bulletin, v. 114, p. 1471–1479, doi:10.1130/0016-7606(2002)114<1471:COTAAO>2.0.CO;2.

Grove, K., 1993, Latest Cretaceous basin formation within the Salinian terrane of west-central California: Geological Society of America Bulletin, v. 105, p. 447–463, doi:10.1130/0016-7606(1993)105<0447:LCBFWT>2.3.CO;2.

Grove, M., Jacobson, C.E., Barth, A.P., and Vucic, A., 2003a, Temporal and spatial trends of Late Cretaceous–Early Tertiary underplating of Pelona and related schists beneath southern California and southwestern Arizona, *in* Johnson, S.E., et al., eds., Tectonic Evolution of Northwestern Mexico and the Southwestern USA: Geological Society of America Special Paper 374, p. 381–406.

Grove, M., Lovera, O.M., and Harrison, T.M., 2003b, Late Cretaceous cooling of the east-central Peninsular Ranges Batholith (33°N): Relationship to La Posta Pluton emplacement, Laramide shallow subduction, and forearc, *in* Johnson, S.E., et al., eds., Tectonic Evolution of Northwestern Mexico and the Southwestern USA: Geological Society of America Special Paper 374, p. 355–379.

Grove, M., Bebout, G.E., Jacobson, C.E., Barth, A.P., Kimbrough, D.L., King, R.L., Zou, H., Lovera, O.M., Mahoney, B.J., and Gehrels, G.G., 2008, The Catalina Schist: Evidence for middle Cretaceous subduction erosion of southwestern North America, *in* Draut, A.E., Clift, P.D., and Scholl, D.W., eds., Formation and Applications of the Sedimentary Record in Arc Collision Zones: Geological Society of America Special Paper 436, p. 335–362.

Gutscher, M.A., Spakman, W., Bijward, H., and Engdahl, E.R., 2000, Geodynamics of flat subduction: Seismicity and tomographic constraints from the Andean margin: Tectonics, v. 19, p. 814–833, doi:10.1029/1999TC001152.

Hall, C.A., Jr., 1991, Geology of the Point Sur–Lopez Point Region, Coast Ranges, California: A Part of the Southern California Allochthon: Geological Society of America Special Paper 266, 40 p.

Hall, C.A., Jr., and Saleeby, J.B., 2013, Salinia revisited: A crystalline nappe sequence lying above the Nacimiento fault and dispersed along the San Andreas fault system, central California: International Geology Review, v. 55, p. 1575–1615, doi:10.1080/00206814.2013.825141.

Henderson, L.J., Gordon, R.G., and Engebretson, D.C., 1984, Mesozoic aseismic ridges on the Farallon plate and southward migration of shallow subduction during the Laramide orogeny: Tectonics, v. 3, p. 121–132, doi:10.1029/TC003i002p00121.

Henry, C.D., Hinz, N.H., Faulds, J.E., Colgan, J.P., John, D.A., Brooks, E.R., Cassel, E.J., Garside, L.J., Davis, D.A., and Castor, S.B., 2012, Eocene–early Miocene paleotopography of the Sierra Nevada–Great Basin–Nevadaplano based on widespread ash-flow tuffs and paleovalleys: Geosphere, v. 8, p. 1–27, doi:10.1130/GES00727.1.

Herzig, C.T., and Kimbrough, D.L., 2014, Santiago Peak volcanics: Early Cretaceous arc volcanism of the western Peninsular Ranges batholith, southern California, *in* Morton, D.M., and Miller, F.K., eds., Peninsular Ranges Batholith, Baja California and Southern California: Geological Society of America Memoir 211, p. 345–364.

Hill, M.L., and Dibblee, T.W., Jr., 1953, San Andreas, Garlock, and Big Pine faults, California: Geological Society of America Bulletin, v. 64, p. 443–458, doi:10.1130/0016-7606(1953)64[443:SAGABP]2.0.CO;2.

House, M.A., Wernicke, B.P., and Farley, K.A., 2001, Paleo-geomorphology of the Sierra Nevada, California, from (U-Th)/He ages in apatite: American Journal of Science, v. 301, p. 77–102, doi:10.2475/ajs.301.2.77.

Hughes, G.R., and Mahood, G.A., 2011, Silicic calderas in arc settings: Characteristics, distribution, and tectonic controls: Geological Society of America Bulletin, v. 123, p. 1577–1595, doi:10.1130/B30232.1.

Ingersoll, R.V., 1979, Evolution of the Late Cretaceous forearc basin, northern and central California: Geological Society of America Bulletin, v. 90, p. 813–826, doi:10.1130/0016-7606(1979)90<813:EOTLCF>2.0.CO;2.

Ingersoll, R.V., 1983, Petrofacies and provenance of late Mesozoic forearc basin, northern and central California: American Association of Petroleum Geologists Bulletin, v. 67, p. 1125–1142.

Ingersoll, R.V., Grove, M., Jacobson, C.E., Kimbrough, D.L., and Hoyt, J.F., 2013, Detrital zircons indicate no drainage link between southern California rivers and the Colorado Plateau from mid-Cretaceous through Pliocene: Geology, v. 41, p. 311–314, doi:10.1130/G33807.1.

Irwin, W.P., and Wooden, J.L., 2001, Map Showing Plutons and Accreted Terranes of the Sierra Nevada, California with a Tabulation of U/Pb Isotopic Ages: U.S. Geological Survey Open-File Report 2001-229, scale 1:1,000,000.

Jacobson, C.E., Oyarzabal, F.R., and Haxel, G.B., 1996, Subduction and exhumation of the Pelona-Orocopia-Rand schists, southern California: Geology, v. 24, p. 547–550, doi:10.1130/0091-7613(1996)024<0547:SAEOTP>2.3.CO;2.

Jacobson, C.E., Grove, M., Pedrick, J.N., Barth, A.P., Marsaglia, K.M., Gehrels, G.E., and Nourse, J.A., 2011, Late Cretaceous–early Cenozoic tectonic evolution of the southern California margin inferred from provenance of trench and forearc sediments: Geological Society of America Bulletin, v. 123, p. 485–506, doi:10.1130/B30238.1.

Johnson, J.D., and Normark, W.R., 1974, Neogene tectonic evolution of the Salinian block, west-central California: Geology, v. 2, p. 11–14, doi:10.1130/0091-7613(1974)2<11:NTEOTS>2.0.CO;2.

Kanter, L.R., and McWilliams, M.O., 1982, Rotation of the southernmost Sierra Nevada, California: Journal of Geophysical Research, v. 87, p. 3819–3830, doi:10.1029/JB087iB05p03819.

Kennedy, M.P., and Moore, G.W., 1971, Stratigraphic relations of Upper Cretaceous and Eocene formations, San Diego coastal area, California: American Association of Petroleum Geologists Bulletin, v. 55, p. 709–722.

Kidder, S., Ducea, M., Gehrels, G., Patchett, P.J., and Vervoort, J., 2003, Tectonic and magmatic development of the Salinian Coast Ridge belt, California: Tectonics, v. 22, no. 5, 1058, doi:10.1029/2002TC0001409, p. 12-1–12-20.

Kies, R.P., and Abbott, P.L., 1982, Sedimentology and paleogeography of Lower Paleogene conglomerates, southern California Continental Borderland, *in* Fife, D.L., and Minch, J.A., eds., Geology and Mineral Wealth of the California Transverse Ranges: South Coast Geological Society Annual Symposium and Guidebook 10, p. 337–349.

Kimbrough, D.L., Smith, D.P., Mahoney, B.J., Moore, T.E., Grove, M., Gastil, R.G., Ortega-Rivera, A., and Fanning, M.C., 2001, Forearc-basin sedimentary response to rapid Late Cretaceous batholith emplacement in the Peninsular Ranges of southern and Baja California: Geology, v. 29, p. 491–494, doi:10.1130/0091-7613(2001)029<0491:FBSRTR>2.0.CO;2.

Kimbrough, D.L., Grove, M., Mahoney, J., Barnard, P., and Keller, B., 2009, Detrital zircon U-Pb geochronology of the modern Sacramento–San Joaquin River delta, California, and implications for interpretation of Late Cretaceous Great Valley Group sandstone provenance: Geological Society of America Abstracts with Programs, v. 41, no. 7, p. 657.

Kimbrough, D.L., Abbott, P.L., Balch, D.C., Bartling, S.H., Grove, M., Mahoney, J.B., and Donohue, R.F., 2014a, Upper Jurassic Peñasquitos Formation—Forearc basin western wall rock of the Peninsular Ranges batholith, *in* Morton, D.M., and Miller, F.K., eds., Peninsular Ranges Batholith, Baja California and Southern California: Geological Society of America Memoir 211, p. 625–644.

Kimbrough, D.L., Grove, M., and Morton, D.M., 2014b, Timing and significance of gabbro emplacement within two distinct plutonic domains of the Peninsular Ranges batholith, Southern and Baja California: Geological Society of America Bulletin, doi:10.1130/B30914.1 (in press).

Kistler, R.W., and Champion, D.E., 2001, Rb-Sr Whole-Rock and Mineral Ages, K-Ar, ^{40}Ar/^{39}Ar, and U-Pb Mineral Ages, and Strontium, Lead, Neodymium, and Oxygen Isotopic Compositions for Granitic Rocks from the Salinian Composite Terrane, California: U.S. Geological Survey Open-File Report 01–453, 84 p.

Kooser, M., 1982, Stratigraphy and sedimentology of the type San Francisquito Formation, southern California, *in* Crowell, J.C., and Link, M.H., eds., Geologic History of Ridge Basin, Southern California: Los Angeles, Pacific Section, SEPM (Society for Sedimentary Geology), p. 53–61.

LaMaskin, T.A., 2012, Detrital zircon facies of Cordilleran terranes in western North America: GSA Today, v. 22, no. 3, p. 4–11, doi:10.1130/GSATG142A.1.

Laskowski, A.K., DeCelles, P.G., and Gehrels, G.E., 2013, Detrital zircon geochronology of Cordilleran retroarc foreland basin strata, western North America: Tectonics, v. 32, p. 1027–1048, doi:10.1002/tect.20065.

Laursen, J., Scholl, D.W., and von Huene, R., 2002, Neotectonic deformation of the central Chile margin: Deepwater forearc basin formation in response to hot spot ridge and seamount subduction: Tectonics, v. 21, 1038, doi:10.1029/2001TC901023, p. 2-1–2-27.

Lechler, A.R., and Niemi, N.A., 2011, Sedimentologic and isotopic constraints on the Paleogene paleogeography and paleotopography of the southern Sierra Nevada, California: Geology, v. 39, p. 379–382, doi:10.1130/G31535.1.

Linn, A.M., DePaolo, D.J., and Ingersoll, R.V., 1992, Nd-Sr isotopic, geochemical, and petrographic stratigraphy and paleotectonic analysis: Mesozoic Great Valley forearc sedimentary rocks of California: Geological Society of America Bulletin, v. 104, p. 1264–1279, doi:10.1130/0016-7606(1992)104<1264:NSIGAP>2.3.CO;2.

Lipman, P.W., 1992, Magmatism in the Cordilleran United States; Progress and problems, *in* Burchfield, B.L., Zoback, M.L., and Lipman, P., eds., The Cordilleran Orogen: Conterminous U.S.: Boulder, Colorado, Geological Society of America, The Geology of North America, v. G-3, p. 107–168.

Liu, L., Spasjevic, S., and Gurnis, M., 2008, Reconstructing Farallon plate subduction beneath North America back to the Late Cretaceous: Science, v. 322, p. 934–938, doi:10.1126/science.1162921.

Liu, L., Gurnis, M., Seton, M., Saleeby, J., Muller, R.D., and Jackson, J.M., 2010, The role of oceanic plateau subduction in the Laramide orogeny: Nature Geoscience, v. 3, p. 353–357, doi:10.1038/ngeo829.

Livaccari, R.F., Burke, K., and Sengor, A.M.C., 1981, Was the Laramide orogeny related to subduction of an oceanic plateau?: Nature, v. 289, p. 276–278, doi:10.1038/289276a0.

Lowe, T.K., 1996, Petrogenesis of the Minarets and Merced Peak Volcanic-Plutonic Complexes, Sierra Nevada, California [Ph.D. thesis]: Stanford, California, Stanford University, 157 p.

Luyendyk, B.P., 1991, A model for Neogene crustal rotations, transtension, and transpression in southern California: Geological Society of America Bulletin, v. 103, p. 1528–1536, doi:10.1130/0016-7606(1991)103<1528:AMFNCR>2.3.CO;2.

Matthews, V., III, 1976, Correlation of Pinnacles and Neenach volcanic fields and their bearing on San Andreas fault problem: American Association of Petroleum Geologists Bulletin, v. 60, p. 2128–2141.

Mattinson, J.M., 1990, Petrogenesis and evolution of the Salinian magmatic arc, *in* Anderson, J.L., ed., The Nature and Origin of Cordilleran Magmatism: Geological Society of America Memoir 174, p. 237–250.

McDowell, F.W., Roldán-Quintana, J., and Connelly, J.N., 2001, Duration of Late Cretaceous–Early Tertiary magmatism in east-central Sonora, Mexico: Geological Society of America Bulletin, v. 113, p. 521–531, doi:10.1130/0016-7606(2001)113<0521:DOLCET>2.0.CO;2.

M'Gonigle, J.W., and Dalrymple, G.B., 1996, ^{40}Ar/^{39}Ar Ages of Challis Volcanic Rocks and the Initiation of Tertiary Sedimentary Basins in Southwestern Montana: U.S. Geological Survey Bulletin 2132, 17 p.

Miller, E.L., Miller, M.M., Wright, J.E., and Madrid, R., 1992, Late Paleozoic paleogeographic and tectonic evolution of the western U.S. Cordillera, *in* Burchfiel, C., Lipman, W., and Zoback, S., eds., The Cordilleran Orogen; Conterminous U.S.: Boulder, Colorado, Geological Society of America, Geology of North America, v. G-3, p. 57–106.

Mitchell, C., Graham, S.A., and Suek, D.H., 2010, Subduction complex uplift and exhumation and its influence on Maastrichtian forearc stratigraphy in the Great Valley Basin, northern San Joaquin Valley, California: Geological Society of America Bulletin, v. 122, p. 2063–2078, doi:10.1130/B30180.1.

Moxon, I.A., 1990, Stratigraphic and Structural Architecture of the San Joaquin and Sacramento Valleys [Ph.D. thesis]: Stanford, California, Stanford University, 371 p.

Moxon, I.W., and Graham, S.A., 1987, History and controls of subsidence in the Late Cretaceous–Tertiary Great Valley forearc basin, California: Geology, v. 15, p. 626–629, doi:10.1130/0091-7613(1987)15<626:HACOSI>2.0.CO;2.

Mulch, A., Graham, S.A., and Chamberlain, C.P., 2006, Hydrogen isotopes in Eocene river gravels and paleoelevation of the Sierra Nevada: Science, v. 313, p. 87–89, doi:10.1126/science.1125986.

Nicholson, C., Sorlien, C.C., Atwater, T., Crowell, J.C., and Luyendyk, B.P., 1994, Microplate capture, rotation of the western Transverse Ranges, and initiation of the San Andreas transform as a low-angle fault system: Geology, v. 22, p. 491–495, doi:10.1130/0091-7613(1994)022<0491:MCROTW>2.3.CO;2.

Nilsen, T.H., and Abbott, P.L., 1981, Paleogeography and sedimentology of Upper Cretaceous turbidites, San Diego, California: American Association of Petroleum Geologists Bulletin, v. 65, p. 1256–1284.

Nilsen, T.H., and Clarke, S.H., Jr., 1975, Sedimentation and Tectonics in the Early Tertiary Continental Borderland of Central California: U.S. Geological Survey Professional Paper 925, 64 p.

Nilsen, T.H., Dibblee, T.W., Jr., and Simoni, T.R., Jr., 1974, Stratigraphy and sedimentology of the Cantua Sandstone Member of the Lodo Formation, Vallecitos area, California, *in* Payne, M., ed., The Paleogene of the Panoche Creek–Cantua Creek Area, Central California: Los Angeles, Pacific Section, SEPM (Society for Sedimentary Geology), Fall Field Trip Guidebook, p. 38–68.

Poldervaart, A., 1956, Zircon in rocks: 2. Igneous rocks: American Journal of Science, v. 254, p. 521–554, doi:10.2475/ajs.254.9.521.

Premo, W., Morton, D.M., Snee, L., Naeser, N.D., and Fanning, C.M., 1998, Isotopic ages, cooling histories, and magmatic origins for Mesozoic tonalitic plutons from the N. Peninsular Ranges batholith, S. California: Geological Society of America Abstracts with Programs, v. 30, no. 5, p. 59–60.

Prohoroff, R., Wakabayashi, J., and Dumitru, T.A., 2012, Sandstone matrix olistostrome deposited on intra-subduction complex serpentinite, Franciscan Complex, western Marin County, California: Tectonophysics, v. 568–569, p. 296–305, doi:10.1016/j.tecto.2012.05.018.

Saleeby, J., 2003, Segmentation of the Laramide slab—Evidence from the southern Sierra Nevada region: Geological Society of America Bulletin, v. 115, p. 655–668, doi:10.1130/0016-7606(2003)115<0655:SOTLSF>2.0.CO;2.

Saleeby, J., Farley, K.A., Kistler, R.W., and Fleck, R., 2007, Thermal evolution and exhumation of deep-level batholithic exposures, southernmost Sierra Nevada, California, *in* Cloos, M., Carlson, W.D., Gilbert, M.C., Liou, J.G., and Sorensen, S.S., eds., Convergent Margin Terranes and Associated Regions: A Tribute to W.G. Ernst: Geological Society of America Special Paper 419, p. 39–66, doi:10.1130/2006.2419(01).

Saleeby, J.B., Ducea, M.N., Busby, C., Nadin, E., and Wetmore, P.H., 2008, Chronology of pluton emplacement and regional deformation in the southern Sierra Nevada batholith, California, *in* Wright, J.E., and Shervais, J.W., eds., Ophiolites, Arcs, and Batholiths: A Tribute to Cliff Hopson: Geological Society of America Special Paper 438, p. 397–427.

Saleeby, J.B., Saleeby, Z., Liu, L., and Maheo, G., 2010, Mid-Cretaceous regional exhumation of the Sierra Nevada–Great Valley batholith and a possible tectonic driving mechanism: Geological Society of America Abstracts with Programs, v. 42, no. 4, p. 67.

Schulein, B.J., 1993, Sedimentation and Tectonics of the Upper Lower to Lower Middle Eocene Domengine Formation Vallecitos Syncline, California [M.S. thesis]: Stanford, California, Stanford University, 343 p.

Schweickert, R.A., and Cowan, D.S., 1975, Early Mesozoic tectonic evolution of the western Sierra Nevada, California: Geological Society of America Bulletin, v. 86, p. 1329–1336, doi:10.1130/0016-7606(1975)86<1329:EMTEOT>2.0.CO;2.

Seiders, V.M., and Cox, B.T., 1992, Place of Origin of the Salinian Block, California, as Based on Clast Compositions of Upper Cretaceous and Lower Tertiary Conglomerates: U.S. Geological Survey Professional Paper 1526, 80 p.

Sharman, G.R., Graham, S.A., Grove, M., and Hourigan, J.K., 2013, A reappraisal of the early slip history of the San Andreas fault, central California, USA: Geology, v. 41, p. 727–730, doi:10.1130/G34214.1.

Shaw, S.E., Todd, V.R., and Grove, M., 2003, Jurassic peraluminous gneissic granites in the axial zone of the Peninsular Ranges, southern California, *in* Johnson, S.E., et al., eds., Tectonic Evolution of Northwestern Mexico and the Southwestern USA: Geological Society of America Special Paper 374, p. 157–183.

Silver, L.T., and Chappell, B., 1988, The Peninsular Ranges batholith: An insight into the Cordilleran batholiths of southwestern North America: Transactions of the Royal Society of Edinburgh–Earth Sciences, v. 79, p. 105–121, doi:10.1017/S0263593300014152.

Snow, C.A., Wakabayashi, J., Ernst, W.G., and Wooden, J.L., 2010, Detrital zircon evidence for progressive underthrusting in Franciscan metagraywackes, west-central California: Geological Society of America Bulletin, v. 122, p. 282–291, doi:10.1130/B26399.1.

Spencer, J.E., and Normark, W.R., 1979, Tosco-Abreojos fault zone: A Neogene transform plate boundary within the Pacific margin of southern Baja California: Geology, v. 7, p. 554–557, doi:10.1130/0091-7613(1979)7<554:TFZANT>2.0.CO;2.

Spencer, J.E., Richard, S.M., Gehrels, G.E., Gleason, J.D., and Dickinson, W.R., 2011, Age and tectonic setting of the Mesozoic McCoy Mountains Formation in western Arizona, USA: Geological Society of America Bulletin, v. 123, p. 1258–1274, doi:10.1130/B30206.1.

Sullivan, R., and Sullivan, M.D., 2012, Sequence stratigraphy and incised valley architecture of the Domengine Formation, Black Diamond Mines Regional Preserve and the southern Sacramento basin, California, U.S.A.: Journal of Sedimentary Research, v. 82, p. 781–800, doi:10.2110/jsr.2012.66.

Sundberg, F.A., and Cooper, J.D., 1982, Late Cretaceous (Campanian) paleogeography of southern California, *in* Bottjer, D.J., Coldburn, I.P., and Cooper, J.D., eds., Late Cretaceous Depositional Environments and Paleogeography, Santa Ana Mountains, Southern California: Lose Angeles, Pacific Section, SEPM (Society for Sedimentary Geology), Field Trip Volume and Guidebook, p. 115–121.

Surpless, K.D., and Beverly, E.M., 2013, Understanding a critical basinal link in Cretaceous Cordilleran paleogeography: Detailed provenance of the Hornbrook Formation, Oregon and California: Geological Society of America Bulletin, v. 125, p. 709–727, doi:10.1130/B30690.1.

Tarduno, J.A., McWilliams, M., Debiche, M.G., Sliter, M.V., and Blake, M.C., Jr., 1985, Franciscan Complex caldera limestones: Accreted remnants of Farallon plate oceanic plateaus: Nature, v. 317, p. 345–347, doi:10.1038/317345a0.

Todd, V.R., Shaw, S.E., and Hammarstrom, J.M., 2003, Cretaceous plutons of the Peninsular Ranges batholith, San Diego and westernmost Imperial Counties, California: Intrusion across a Late Jurassic continental margin, *in* Johnson, S.E., et al., eds., Tectonic Evolution of Northwestern Mexico and the Southwestern USA: Geological Society of America Special Paper 374, p. 185–235.

Underwood, M.B., 1983, Depositional setting of the Paleogene Yager Formation, northern Coast Ranges of California, *in* Larue, D.K., and Steel, R.J., eds., Cenozoic Marine Sedimentation, Pacific Margin, U.S.A.: Los Angeles, Pacific Section, Society of Economic Paleontologists and Mineralogists, p. 81–101.

Underwood, M.B., and Moore, G.F., 1995, Trenches and trench-slope basins, *in* Busby, C.J., and Ingersoll, R.V., eds., Tectonics of Sedimentary Basins: Cambridge, Massachusetts, Blackwell Science, p. 179–219.

Von Huene, R., and Scholl, D.W., 1991, Observations at convergent margin concerning sediment subduction erosion, and the growth of continental crust: Reviews of Geophysics, v. 29, p. 279–316, doi:10.1029/91RG00969.

Walawender, M.J., Gastil, R.G., Clinkenbeard, J.P., McCormick, W.V., Eastman, B.G., Wernicke, R.S., Wardlaw, M.S., Gunn, S.H., and Smith, B.M., 1990, Origin and evolution of the zoned La Posta–type plutons, eastern Peninsular Ranges batholith, southern and Baja California, *in* Anderson, J.L., ed., The Nature and Origin of Cordilleran Magmatism: Geological Society of America Memoir 174, p. 1–18.

Walker, J.D., Martin, M.W., and Glazner, A.F., 2002, Late Paleozoic to Mesozoic development of the Mojave Desert and environs, California, *in* Glazner, A.F., Walker, J.D., and Bartley, J.M., eds., Geologic Evolution of the Mojave Desert and Southwestern Basin and Range: Geological Society of America Memoir 195, p. 1–18.

Watson, E.B., 1979, Zircon saturation in felsic liquids: Experimental results and applications to trace element geochemistry: Contributions to Mineralogy and Petrology, v. 70, p. 407–419, doi:10.1007/BF00371047.

Wells, M.L., and Hoisch, T.D., 2008, The role of mantle delamination in widespread Late Cretaceous extension and magmatism in the Cordilleran orogen, western United States: Geological Society of America Bulletin, v. 120, p. 515–530, doi:10.1130/B26006.1.

Wernicke, B.P., 1992, Cenozoic extensional tectonics of the U.S. Cordillera, *in* Burchfiel, B.C., Lipman, P.W., and Zoback, M.L., eds., The Cordilleran Orogen: Conterminous U.S.: Boulder, Colorado, Geological Society of America, Geology of North America, v. G-3, p. 553–581.

Williams, T.A., 1997, Basin-Fill Architecture and Forearc Tectonics: Cretaceous Great Valley Group, Sacramento Basin, Northern California [Ph.D. thesis]: Stanford, California, Stanford University, 412 p.

Williams, T.A., and Graham, S.A., 2013, Controls on forearc basin architecture from seismic and sequence stratigraphy of the Upper Cretaceous Great Valley Group, central Sacramento basin, California: International Geology Review, v. 55, p. 2030–2059, doi:10.1080/00206814.2013.817520.

Williams, T.A., Graham, S.A., and Constenius, K.N., 1998, Recognition of a Santonian submarine canyon, Great Valley Group, Sacramento basin, California: Implications for petroleum exploration and sequence stratigraphy of deep-marine strata: American Association of Petroleum Geologists Bulletin, v. 82, p. 1575–1595.

Science Editor: Christian Koeberl
Associate Editor: Carl Jacobson

Manuscript Received 10 January 2014
Revised Manuscript Received 15 May 2014
Manuscript Accepted 6 May 2014

Printed in the USA